

# Local environmental context drives heterogeneity of early succession dynamics in alpine glacier forefields

Arthur Bayle<sup>1†\*</sup>, Bradley Z. Carlson<sup>2†</sup>, Anaïs Zimmer<sup>3</sup>, Sophie Vallée<sup>4</sup>, Antoine Rabatel<sup>5</sup>, Edoardo Cremonese<sup>6</sup>, Gianluca Filippa<sup>6</sup>, Cédric Dentant<sup>7</sup>, Christophe Randin<sup>8</sup>, Andrea Mainetti<sup>9</sup>, Erwan Roussel<sup>10</sup>, Simon Gascoin<sup>11</sup>, Dov Corenblit<sup>10</sup> & Philippe Choler<sup>1</sup>

<sup>1</sup>Univ. Grenoble Alpes, Univ. Savoie Mont Blanc, CNRS, LECA, F-38000 Grenoble, France

<sup>2</sup>Centre de Recherches sur les Écosystèmes d'Altitude (CREA), Observatoire du Mont-Blanc, F-74400 Chamonix, France

<sup>3</sup>Department of Geography and the Environment, The University of Texas at Austin, Austin, Texas, USA

<sup>4</sup>Conservatoire Botanique National Alpin (CBNA), F-73000 Chambéry, France

<sup>5</sup>Univ. Grenoble Alpes, CNRS, IRD, Grenoble-INP, Institut des Géosciences de l'Environnement (IGE, UMR 5001), F-38000 Grenoble, France

<sup>6</sup>Environmental Protection Agency of Aosta Valley, Climate Change Unit, Loc. La Maladière, 48, IT-11020 Saint Christophe (AO), Italy

<sup>7</sup>Parc National des Ecrins, Domaine de Charance, Gap, France

<sup>8</sup>Univ. Lausanne, Dept. of Ecology & Evolution / Interdisciplinary Centre for Mountain Research (CIRM), Biopore, CH-1015 Lausanne, Switzerland

<sup>9</sup>Biodiversity Service and Scientific Research, Gran Paradiso National Park, Torino, Italy

<sup>10</sup>Université Clermont Auvergne, CNRS, GEOLAB, Clermont-Ferrand, France

<sup>11</sup>CESBIO, Université de Toulouse, CNES/CNRS/IRD/INRAE/UPS, Toulouse, France

\*These authors contributed equally to this work

Correspondence to: Arthur Bayle (arthur.bayle.env@gmail.com)

**Abstract.** Glacier forefields have long provided ecologists with a model to study patterns of plant succession following glacier retreat. While plant survey-based approaches applied along chronosequences provide invaluable information on plant communities, the “space-for-time” approach assumes environmental uniformity and equal ecological potential across sites and does not account for spatial variability in initial site conditions. Remote sensing provides a promising avenue for assessing plant colonisation dynamics using a so-called “real-time” approach. Here, we combined 36 years of Landsat imagery with extensive field sampling along chronosequences of deglaciation for eight glacier forefields in the south-western European Alps to investigate the heterogeneity of early plant succession dynamics. Based on the two complementary and independent approaches, we found strong variability in the time lag between deglaciation and colonisation by plants and in subsequent growth rates, and in the composition of early plant succession. All three parameters were highly dependent on the local environmental context, i.e., neighbouring ~~local~~ cover surrounding the forefields and energy availability linked to temperature and snowmelt gradients. Potential geomorphological disturbance did not emerge as a strong predictor of succession parameters, perhaps due to insufficient spatial resolution of predictor variables. Notably, the identity of pioneer plant species was highly variable, and initial plant community composition had a much stronger influence than elapsed time on since deglaciation showed no consistent relationship to plant assemblages ~~than elapsed time since deglaciation, i.e., we did not identify a consistent identity of pioneer species or order of successional species across forefields as a function of time~~. Overall, both approaches converged towards the conclusion that early plant succession is not stochastic as previous authors have suggested but rather determined by local ecological context ~~is~~. We discuss the importance of scale in deciphering the unique complexity of plant succession in glacier forefields and provide recommendations for improving botanical field surveys and using Landsat time series in glacier forefields systems. Our work demonstrates complementarity between remote sensing and field-based approaches for both understanding and predicting future patterns of plant succession in glacier forefields.

## 1 Introduction

Glaciers in the European Alps began to retreat around the mid-19th century in response to changes in climate conditions driven first by shifts in precipitation (Vincent et al., 2005) and then by human-induced changes in aerosol concentrations in the atmosphere combined with warming (Painter et al., 2013, Sigl et al., 2018). Pronounced glacier retreat marked the end of the Little Ice Age (LIA), a multi-century period during which glacier terminal moraines were up to a few kilometers down valley from their current location (Matthews and Briffa, 2005, Gardent et al., 2014). As glaciers retreat, the surface area of the glacier forefields (i.e., the area extending between the glacier snout and the moraine deposited during the LIA maximum extent) increases (Marta et al., 2021). Over the 20th century, the pace of glacier retreat in the Alps was ~~variable and not constant, with and punctuated by a few brief~~ variable and not constant, with and punctuated by a few brief short glacier advances. However, this ~~variability phase has given way~~ variability phase has given way ~~was recently followed by more to~~ was recently followed by more to consistent and accelerating melting since the 1990s (Vincent et al., 2014), in response to warming air temperatures and associated reductions in snowpack depth and duration (Gobiet et al., 2014). In this context, recently deglaciated areas constitute particularly dynamic ecosystems that are reshaping high mountain landscapes (Haeberli et al., 2017) and associated biodiversity and ecosystem services (Cauvy-Fraunie and Dangles, 2019, Ficetola et al., 2021). These emerging ecosystems have been identified as hotspots of the widespread greening observed throughout the European Alps during recent decades (Bayle, 2020, Choler et al., 2021, Carlson et al., 2017; Dentant et al. 2022), calling for the need to better understand plant colonization dynamics in glacier forefields to predict future trajectories of alpine ecosystems (Huss et al., 2017).

Glacier forefields have long provided ecologists with a model to study patterns of plant succession along chronosequences of glacier retreat (Chapin et al., 1994), most often using a “space-for-time” approach (Pickett, 1989, Zimmer et al., 2018). This method ~~uses the position of plant surveys to estimate time since deglaciation and~~ uses relies on the assumption that within a glacier forefield, initial environmental conditions are consistent, and that pioneer species benefit from equal opportunity for establishment and growth over space and time (Johnson and Miyanishi, 2008). However, field observations accompanied by a growing body of literature indicate that this approach is overly simplistic given the environmental heterogeneity of glacier forefields as well as the complexity of biological processes involved. Indeed, we now know that plant succession rates and trajectories are controlled by both abiotic and biotic processes, which in turn depend on regional landscape and local environmental factors, such as micro-climate (Joly and Brossard, 2007), substrate and disturbance regimes (Anthelme et al., 2021, Eichel et al., 2016), water and nutrient availability (Górniak et al., 2017), micro-topography (Raffl et al., 2006, Scherrer and Körner, 2011) and broad scale gradients such as elevation and continentality (Garibotti et al., 2011, Rydgren et al., 2014, Robbins and Matthews, 2010, Robbins and Matthews, 2014). All these factors can lead to strong heterogeneity in vegetation dynamics within and between glacier forefields.

Plant succession dynamics in glacier forefields, as elsewhere, can be broken down into three fundamental steps (Bradshaw, 1993): (i) diaspores reaching areas of bare ground, i.e., dispersal, (ii) successful and persistent establishment, and (iii) plant succession, as community composition matures and develops over time. Wojcik et al. (2021) recently proposed a novel conceptual model aimed at better understanding and predicting contrasting trajectories of plant succession dynamics in glacier forefields based on the complex interplay between autogenic factors, i.e., time dependent biological succession, and allogenic factors, i.e., external environmental factors such as climate or geomorphological disturbances. The authors suggest that the importance of autogenic and allogenic components varies over time, with an initial stochastic phase (i.e., dispersal) followed by a more deterministic phase defined by environmental factors, biological interactions, and bio-geomorphic feedbacks (Eichel et al., 2016). Contrasting succession trajectories within glacier forefields are presented as the result of variations in (i) time since glacier retreat; (ii) initial site conditions (heterogeneous micro-climate, substrate properties and resource availability); and (iii) geomorphological disturbances (hillslope, torrential, periglacial, aeolian disturbances). In addition to time,

autogenic biological properties also shape plant succession dynamics: regional species pool composition determines propagule pressure, while plant functional traits (wind dispersal and low seed mass) facilitate the arrival and establishment of pioneer species (Franzén et al., 2019, Rosero et al., 2021, Schumann et al., 2016). At broader scales, variability in plant succession rates between glacier forefields has been linked to elevation and continentality, which in turn influence more direct environmental parameters such as temperature and snow cover duration (Robbins and Matthews, 2010).

In addition to assuming environmental uniformity and equal ecological potential over space, plant survey-based approaches applied along chronosequences yield only a snapshot of plant community properties and fail to provide insights into the temporal dynamics of succession. To address questions linking auto- and allogenic factors to time lags, i.e., time between a surface deglaciation and its initial plant establishment, it appears necessary to adopt a “real-time” approach based on annually resolved information on plant succession dynamics. While some studies have successfully implemented repeat surveys of permanent plots in the context of glacier forefields (Fickert and Grüniger, 2018) repeat field surveys of plant communities in often remote and hard-to-access mountain environments present major challenges in terms of cost and effort.

As a complementary approach to traditional plot-based surveys, which remain essential to understand geomorphological/biogeomorphic processes on the ground, remote sensing provides a promising avenue for assessing plant colonization dynamics within and between glacier forefields using a so-called “real-time” approach. Beginning in 1984 with the Landsat 5 TM, followed by Landsat 7 ETM+ and Landsat 8 OLI sensors, Landsat satellites currently provide a 36-year archive of 30 m resolution images acquired at 16-day intervals over the globe’s terrestrial areas. Availability of Landsat imagery since the mid-1980s allows for investigating plant succession dynamics since the most recent observed advance of alpine glaciers and in response to accelerating glacier retreat during recent decades. Vegetation indices such as the Normalized Difference Vegetation Index (NDVI) provide a proxy of plant biomass (Tucker and Sellers, 1986), photosynthetic activity and vegetation cover and have the potential to reliably quantify plant succession in rocky areas with low plant cover. As NDVI is a non-physical and uni-dimensional quantity based on remotely measured reflectance, variations in quantities over time can be disconnected from changes in plant cover on the ground, particularly in the context of heterogeneous topography (Bayle et al., 2021). In addition to systematic errors caused by sensor limitations, variation in NDVI over time can be due to atmospheric and cloud contamination (Masek et al., 2006), angular effects due to variation in sun-surface-sensor geometry or topography (Nagol et al., 2015, Martín-Ortega et al., 2020), sensor degradation and calibration changes (Markham and Helder, 2012) or between sensor spectral band pass (Steven et al., 2003). Overall, it has been shown that NDVI increases near-linearly with fractional vegetation cover (horizontal density) until values reach between 80% and 90% at which point it tends to saturate and increases slowly with increasing Leaf Area Index (vertical density). Remote sensing approaches have already been used efficiently in the context of glacier forefields (Klaar et al., 2015, Fischer et al., 2019, Bayle, 2020, Knoflach et al., 2021) and high sensitivity of Landsat-based NDVI to low plant cover has been demonstrated in glacier forefields (Bayle et al., 2021) and in Antarctica (Fretwell et al., 2011).

Here, we investigated early plant succession dynamics (0-35 years since glacier retreat) in the context of eight glaciers distributed across the southwestern European Alps. Specifically, we sought to answer the following ecological questions: (1) Is observed heterogeneity in early plant succession dynamics (Time between deglaciation and plant colonisation, and plant growth rate following colonization) indeed purely stochastic or can this variability be linked to environmental factors? (2) Is early plant community composition consistent across sites and shaped by time availability or heterogeneous and driven by local environmental context? To address these questions, we utilized two independent data sources: 36 years of Landsat imagery and 297 floristic field plots. First, we derived two indicators of vegetation dynamics from Landsat time series, which are (i) time lag between ice melting and detection of plant colonisation/establishment, and (ii) plant growth rate following colonization/establishment. Then, we investigated the spatial heterogeneity of these indicators and their respective drivers

114 using proxies of the local environmental and geomorphological context (allogenic factors). Second, we assessed turnover in plant community  
115 composition between and within the eight glacier forefields using a “space-for-time” approach and with regard to local environmental and  
116 geomorphological context (allogenic factors) and time since deglaciation (autogenic factor). Finally, we questioned the capacity of field  
117 sampling to capture heterogeneity in vegetation dynamics with respect to spatially exhaustive remote sensing approach, and we provide  
118 some recommendations to improve field sampling methodology for future studies. In addition to testing theoretical expectations in glacier  
119 forefields across a broad spectrum of environmental and ecological contexts, our study provides for the first time a clear roadmap for applying  
120 widely available remote sensing data to quantify and improve our understanding of trajectories of plant colonization and succession in glacier  
121 forefields.

## 123 **2 Data and study site**

### 124 *2.1 Study site*

125 Our study investigates eight glacier forefields distributed throughout the southwestern European Alps (Figure 1) in France (Glacier  
126 Blanc, Saint-Sorlin, Gébroulaz, Tour and Pélerins), Switzerland (Orny) and Italy (Lavassey and Lauson). Sites are distributed from 45° to  
127 46° N and from 6° to 7° E across a variety of slopes and aspects, and elevations. Substrates are highly variable both within and between  
128 forefields including exposed bedrock, chaotic blocks of various sizes, gravel, and sand. Stream networks are often intricate, with strong  
129 seasonal and daily variability.

### 131 *2.2 Age of deglaciation*

132 Chronosequences of glacier outlines for the eight glaciers were initially obtained from various sources depending on the country.  
133 For France (GB, GEB, STS, PEL, TR), glacier outlines were extracted from the GLIMS database (Gardent et al. 2014) which contain outlines  
134 dating from 1985/86 based on Landsat 5 TM (30m), 2003 based on Landsat 5 TM and 7 ETM+ (30m), 2006, 2008 or 2009 (depending on  
135 the glacier) based on sub-meter resolution images from BD ORTHO IGN and finally 2014, 2016, 2018 (depending on the glacier) Spot 6/7  
136 images (1.5 m). For Italy (LAU, LAV), glacier outlines for 1975 were obtained based on photo interpretation of Regional Technical Maps,  
137 1999, 2005, 2012 and 2019 based on orthophoto (50 cm) and Sentinel-2 (10 m). For Switzerland (OR), glacier outlines were extracted from  
138 the GLAMOS database (Linsbauer et al., 2021). Overall, we were able to obtain chronosequences for the eight glaciers that approximately  
139 corresponded to the Landsat time series historical depth. As our glacier contours database mixed automatic and manual methods with sources  
140 at medium to high resolution, important quality differences were observed within and between glacier chronosequence as older contours  
141 were mostly based on coarse resolution images through automatic approaches that tend to perform poorly for debris-covered glaciers. To  
142 improve the consistency of our database and the reliability of further analysis, we carried out manual ~~photo interpretation~~photo interpretation  
143 of sub-meter historical images for all glacier contours. For STS, TR, OR and LAV, small corrections were applied due only to the  
144 improvement of sources resolution, while for GEB, PEL and LAU, which are totally or partly covered by debris, we substantially improved  
145 the delimitation by accounting for emissary streams, crevasses and lateral scree reoriented by glacier movement. For GB, we also identified  
146 a large section of dead-ice that detached from the main glacier in 2014, and which remains in 2021 (Bayle, 2020). We removed this area  
147 from further analysis. Image sources are presented in Table S2 while detailed procedures to obtain our sub-meter glacier contours database  
148 are presented for each glacier in Figures S1 to S6. Glacier outlines were manually delineated using ArcGIS software (Esri, 10.4.1). A detailed  
149 description of the sources used to improve the glacier outlines dataset can be found in Table S1.

We estimated continuous years of deglaciation (YOD) from glacier outlines using an interpolation method initially designed for the creation of hydrologically corrected digital elevation models (DEMs). We used the Topo-to-raster function in ArcGIS based on the ANUDEM program (Hutchinson et al., 2011), which is specifically designed to work with line features as input, to obtain a raster indicating the YOD. Linear interpolation assumes that glaciers retreated at a constant rate between two dated glacier extents. To evaluate this assumption, interpolated surfaces from Glacier Blanc were compared to a denser chronosequence of deglaciation from Bayle (2020) that were not used in this work. The linear model between the results from interpolation and ground-truth observation obtained a  $R^2$  of 0.945 with a mean error of  $\pm 2$  years (Figure S7).

### 2.3 Vegetation field surveys

Glacier forefields of GB, GEB, STS, PEL, TR, LAV, LAU and OR were surveyed in the months of July and August in 2019 and 2020. For each forefield and chronosequence band (for example the zone deglaciated between 1983 to 2003), we generated a set of 15 random sampling points, while ensuring a minimum distance of five meters between sampling points. In the field we went as close as possible to these points using a GPS and excluded sites that were too dangerous to access walking or that were under water or snow. For each plot, within a 2x2m quadrat we surveyed the percent cover of vascular plants, mosses and lichens, biological soil crust (Khedim et al., 2021, Breen and Lévesque, 2008), and bare ground (which was further subdivided into percent bedrock, sand, gravel  $< 2$  cm, rocks between 2 and 20 cm and blocks larger than 20 cm in diameter). We also recorded all vascular plant species as well as their relative cover and average vegetative height within the quadrat. We had a total of 297 plots with 59, 37, 36, 38, 27, 20, 28 and 52 plots for GB, GEB, LAU, LAV, OR, PEL, STS and TR respectively.

### 2.4 Remote sensing data

Landsat 5 TM, Landsat 7 ETM+ and Landsat 8 OLI standard level 1 Terrain-corrected (L1T) orthorectified images from Collection 1 (geolocation error  $< 12$  m) between 1984 and 2019 for 4 path/row (tiles) were downloaded from the Landsat Earth Explorer data portal (<http://earthexplorer.usgs.gov>) at surface reflectance level of correction. Images with average cloud cover  $< 80\%$  only were selected as high cloud cover can reduce the number of available ground control points and therefore the geolocation accuracy, and because cloud masking relies on clear-sky pixels to identify clouds. As a result, a total of 2846 scenes were selected, 60% of which were from Landsat 5. To improve the robustness of our remote sensing analysis, we applied state of the art methods to correct for inter-sensor spectral variation, Bidirectional Reflectance Distribution Function (BRDF) and illumination related errors, and to mask cloud and cloud shadow cover in mountainous context.

We applied the L7/L8 correction method described by Roy et al. (2016a) to our data to align L8 reflectance to L7. No correction was applied on L5 or L7 as it was shown that the surface reflectance products from Landsat Ecosystem Disturbance Adaptive Processing System (LEDAPS) are consistent through time, with no difference before and after the 2003 ETM+ Scan-Line Corrector (SLC) failure. The BRDF effects due to changes in solar and viewing zenith angle were corrected using the c-factor approach (Roy et al., 2016b) based on the RossThick-LiSparse BRDF model (Schaaf et al., 2002) and using an optimal normalised solar zenith angle defined by Zhang et al. (2016). We applied the Sun-Canopy-Sensor + C model (Soenen et al., 2005) on the recommendation of Sola et al. (2016) to correct for illumination conditions variation due to slope and aspect. Finally, clouds were masked for each scene using the MFmask 4.0 algorithm (<https://github.com/gersl/fmask>) using the default DEM and a cloud probability threshold of 40%. This version has improved clouds and cloud shadows detection by integrating auxiliary data, new cloud probabilities and novel spectral-contextual features, which was crucial in

mountainous area where integration of global DEM to normalise thermal and cirrus bands is necessary (Qiu et al., 2017, Qiu et al., 2019a, Qiu et al., 2019b, Zhu and Woodcock, 2014, Zhu and Woodcock, 2012). Masks were computed for cloud probability threshold of 10%, 40% and 70% for a Landsat 7 ETM+ scene (195-029, captured the 16/07/2019) and visually compared to Fmask 3.3 (Figure S8). The probability of 40% offered good compromise between omission and commission errors and was thus selected. A detailed correction workflow is available in supplementary materials.

To assess vegetation changes at pixel-scale over the eight glacier forefields, we computed the NDVI as follows:

$$NDVI = \frac{(R_{NIR} - R_{Red})}{(R_{NIR} + R_{Red})}$$

where  $R_{NIR}$  and  $R_{Red}$  are the Normalised BRDF-adjusted and topographically corrected reflectance in the NIR and Red bands, respectively. Then, we computed the NDVI annual maximum (NDVImax) available from 01 June to 31 August (day of year ~ 152 to 243) from 1984 to 2019 to obtain a time series of an indicator of vegetation state at 30-m scale. [As shown by Berner et al \(2020\), it is challenging to reliably estimate annual NDVImax using Landsat since these estimates are sensitive to the number of cloud- and snow-free observations acquired each summer. Annual number of usable summer observations increased from 1984 to 2019, with typically few usable summer observations during the 1980s and 1990s \(Zhang et al. 2022\). This bias results in a systematic underestimation of NDVImax when few observations are available \(Figure S9\).](#) To prevent related errors in NDVI trend estimation, a year is discarded from the pixel time series if the mean day of year is superior/inferior to  $\pm 2\sigma$  of the entire time series [as described in Bayle et al \(2022\)](#) (Fig. S10).

### 3. Statistical analysis

Our data analysis workflow is based on using very high resolution chronosequence of deglaciation, Landsat time series and vegetation surveys to derive three “early succession dynamics indicators”. The heterogeneity of these indicators will be explored based on “predictor variables” divided in two categories: the local environmental context and potential geomorphological disturbances. These analyses intend to better understand the deterministic vs. stochastic nature of early succession dynamics in the theoretical framework proposed by Wojcik et al. (2020). [The cComplete workflow is presented in Figure 2.](#)

#### 3.1. Remote sensing-based indicators of succession dynamics

Based on the NDVImax time series, we characterized the proglacial vegetation dynamics at Landsat pixel-scale using two indicators. The (i) Time Lag ( $TL_{NT}$ ), i.e., the number of years between the Year of Deglaciation (YOD) and the year where the NDVI threshold (NT) is exceeded ( $YO_{ENT}$ ), and the (ii) Growth Rate ( $GR_{NT}$ ), i.e., the NDVImax trends computed from the  $YO_{ENT}$  to the last year of the Landsat time series. Ideally, we would compute both indicators for a NT that could identify the year of colonization by vegetation, but as NDVI tends to show noise unrelated to vegetation and that plant establishment is a progressive phenomenon occurring at small scale compared to pixel scale, such a threshold does not exist. Thus, we selected a NT based on Bayle et al. (2021). By comparing Landsat NDVI values to intra-pixel vegetation cover derived from Unmanned Aerial Vehicle (UAV) image, they showed, for example, that a value of 0.071 efficiently discriminates pixels around 5% of vegetation cover (F-score > 0.75) with best efficiency with a value of 0.1 to discriminate with more and less than 13% of vegetation cover (F-score > 0.85). Based on this work, we used an NT of 0.075 as it was a good compromise between specificity and sensitivity regarding plant cover.

Thus, we used  $TL_{0.075}$  and  $GR_{0.075}$  to quantify heterogeneity of intra- and inter-glacier forefield succession dynamics. To consider a year as the one where the NT is exceeded, the NDVI of the two previous years must be lower, and the two next years to be higher. Their-

223 Sen trend estimator was applied for  $GR_{0.075}$  estimation as it is resistant to outliers in short or noisy series (Eastman et al., 2009). An example  
224 of an NDVI time series and all associated data is shown in Figure 3A. We evaluated our method by comparing plant cover (%) obtained  
225 from field sampling between plots identified as vegetated or unvegetated. Finally, as the Landsat time series is limited to the last 40 years,  
226 there is a bias in the  $TL_{0.075}$  value as it is directly constrained by the YOD. For example, a pixel deglaciated in 2010 could only be colonized  
227 in the 9 following years, thus limiting the absolute value of  $TL_{0.075}$  between 1 and 9 years. To bypass this bias, we computed the anomalies  
228 of  $TL_{0.075}$  and  $GR_{0.075}$  as a function of YOD, which is a more relevant measure of heterogeneity in succession dynamics across the eight  
229 glacier forefields (Fig. 3B and 2C).

230 Finally, we implemented two random forest classification analyses to assess relationships between anomalies of  $TL_{0.075}$  and  $GR_{0.075}$   
231 and predictors (Breiman, 2001). We classified the two indicators into three categories: positive anomalies (anomalies of  $TL_{0.075} | GR_{0.075} >$   
232 0), negative anomalies (anomalies of  $TL_{0.075} | GR_{0.075} < 0$ ) and no vegetation detected. For  $TL$ , it resulted in 337, 374 and 1977 samples for  
233 positive, negative and no detection, respectively, and for  $GR$ , 441, 288 and 1959 samples for positive, negative and no detection, respectively.  
234 Only 337 and 288 samples were conserved for  $TL$  and  $GR$ , respectively, to equalize the sample size of each class.

235 Predictors variables included (i) elevation, (ii) local vegetation and (iii) snow-free growing degree days (SF-GDD) to represent the  
236 environmental context (allogenic factors) of the glacier forefields. Elevation was obtained from the 25-m resolution European Digital  
237 Elevation Model (EU-DEM, version 1.1; <https://land.copernicus.eu/imagery-in-situ/eu-dem/>). Snow-free growing degree days (SF-GDD)  
238 maps were calculated through the combined use of the Snow-melt out date (SMOD) product at 20-m resolution derived from Sentinel-2 time  
239 series analysis (Gascoin et al., 2019, Barrou Dumont et al., 2021), and the SAFRAN-CROCUS climatological model from Météo-France  
240 (Vernay et al., 2022), which provides the average daily temperature for each French massif and for 300 m elevation bands (for Swiss and  
241 Italian sites, we applied data from the French Mont-Blanc and Vanoise massifs, respectively). To obtain the SF-GDD for each plot, we  
242 computed the cumulative sum of daily average air temperature above 0°C between snow melt-out date and August 1 for the year 2019. SF-  
243 GDD is representative of the heat accumulated by vegetation during the growing season and is known to be a key variable for habitat  
244 distribution and alpine plant community properties (Choler, 2015, Choler, 2018, Carlson et al., 2015). We defined local vegetation  
245 surrounding the glacier forefield as the expected local vegetation productivity (NDVImax) for a given elevation outside of the glacier  
246 forefield, which we considered to be a proxy of the vegetation proximity and type. To compute this indicator for each plot, we averaged the  
247 NDVImax of the year of deglaciation for the 100-m elevational bands of the plot within a radius of 500-m and by excluding pixels within  
248 the glacier forefield.

249 We also calculated (i) Flow accumulation and (ii) LS-factor (slope length and steepness-Factor) to represent potential  
250 geomorphological disturbances (allogenic factors). The LS factor was derived from the EU-DEM and computed using the original equation  
251 proposed by Desmet and Govers (1996). It combined the S-factor, which accounts for slope angle, and the L-factor that defines slope length.  
252 The combined LS-factor describes the effect of topography on soil erosion and thus is a proxy of “potential” instability due to gravity-related  
253 processes. Flow accumulation was also derived from the EU-DEM and computed using a Multiple Flow Direction algorithm. Both the LS-  
254 factor and Flow accumulation were computed in SAGA (Conrad et al., 2015).

255 We screened highly correlated variables ( $r^2 > |0.7|$ ) by computing pairwise correlations. We then removed elevation as it was highly  
256 correlated to SF-GDD ( $r^2 = -0.73$ ) and Local vegetation ( $r^2 = -0.84$ ). Next, we randomly partitioned the data set into sets for model training  
257 (two-thirds) and evaluation (one-third), and then fit random forest models to optimize out-of-bag classification accuracy. We reassessed the  
258 classification accuracy using the data withheld for model evaluation. We repeated this operation 100 times. Lastly, we computed predictor  
259 importance using the mean decrease in accuracy metric. Predictor importance was calculated using a permutation-based importance measure  
260 where one measures the effect of reshuffling each predictor on model accuracy. Finally, we generated partial dependence plots for the first

variable in terms of importance as defined above to assess how class-specific classification probabilities varied across the range of the predictor while holding all other predictors at their average value. The distribution of predictors was constrained to regions with enough data given that partial dependence plots tend to overinterpret regions with few observations. We used the random Forest, caret, and pdp R packages to implement random forest models and to evaluate their performance (Liaw and Wiener, 2002, Greenwell, 2017).

### 3.2. Heterogeneity of succession dynamics and drivers

To model succession dynamics from the floristic data, we used Non-metric Multidimensional Scaling (NMDS) to perform an unconstrained ordination of the plot by species table. NMDS is a rank-order based multivariate technique that is particularly robust to identify a few important axes of floristic variations in community composition data (Minchin, 1987). We first discarded species with less than five occurrences to limit the proportion of sites with no shared species, as this may complicate the ordination. The resulting table included a total of 297 plots and 119 species. Absolute ~~cover of plant species~~~~species covers~~ ~~were~~ transformed into relative species covers using the Wisconsin standardisation, where species covers are first standardised by maxima and then site covers by maxima. Finally, ~~we calculated the square root of relative plant cover for each species and for each plot~~~~the species covers were square-rooted~~. These transformations are commonly found to improve the results of the NMDS (Legendre and Gallagher, 2001). We ~~then~~ computed a distance matrix using the Bray-Curtis dissimilarity index on transformed species cover ~~with 2 dimensions and 20 minimum random starts iterated two times~~. To avoid local minima, we performed several NMDS with random starts and selected the solution with the minimum stress, i.e., the extent to which the distance between sites in the specified number of dimensions differs from original distances. We used a vector fitting approach to test for linear relationships between NMDS site scores and two sets of variables corresponding ~~to time since deglaciation (autogenic factor), to and to~~ allogenic factors ~~including environmental (neighbouring local~~ vegetation ~~cover~~, SFGDD, ~~elevation~~) and geomorphological context (LS-factor, ~~and flow accumulation and~~, coarse debris). To account for spatial autocorrelation, we implemented two ~~g~~Generalized ~~l~~Least ~~s~~quare (GLS) regression models for each variable: one including an autocorrelated error structure and one without. We used the spherical spatial correlation structure estimated by the function corSphere in the nlme package ~~nlme~~ (Pinheiro and Bates, 2022). The best fitting model was selected using the Akaike Information Criterion corrected for small sample size (AICc). For each competing model, we estimated a pseudo-R-squared based on the regression of the variable on the fitted values. NMDS was performed using the metaMDS function of the vegan R package ~~vegan~~ (Oksanen et al., 2020). GLS regression was fitted using ~~with the gls function of the nlme R package nlme~~. Model evaluation was performed with the R package MuMIn (Barton, 2023). In addition to environmental context and potential disturbances regime variables (allogenic factors) presented in section 3.1, we also considered sediment granulometry as measured in the field with floristic data. ~~Using visual estimates of substrate type and cover carried out for each floristic plot, we~~~~visual field observations~~~~it was obtained by~~ ~~calculated~~~~performing~~ a cumulative weighted mean for each plot of grain size (sand < 0.5 cm, gravel < 2 cm, cobbles between 2 and 20 cm and boulders between 20 cm and 1 m in diameter) ~~visually estimated for floristic plots,~~ by assigning the median value for each class and calculating a cumulative weighted mean.

## 4. Results

### 4.1. Vegetation dynamics heterogeneity assessed through remote sensing

Using 36 years of NDVImax obtained from the Landsat time series, we found strong heterogeneity within and between glacier forefields. It took on average 10 years following deglaciation to reach an ~~average~~ NDVI value of 0.075 for GB in comparison with, for

Formatted: Indent: First line: 1.27 cm



example, 27 years for GEB, 17 for TR, 25 for STS, or even no vegetation detected for LAU over the entire period (Fig. 4). Within glacier forefields, plant colonisation rates varied depending on the glacier with GB depicting the highest heterogeneity in NDVI dynamics following deglaciation, and TR being the more homogenous with almost no pixel with an NDVI value under 0.075 after 30 years (Fig. 4). Also, we did not find vegetated pixels for LAU over the study period, which was corroborated by low plant cover recorded in the 2019 field survey (on average 4%). By simply considering pixels as colonised by plants or not, we found that after 30 years since deglaciation 80% of GB, TR, and STS forefields were colonised, and only 30% for PEL and LAV (Fig. 5). Overall, considering anomalies of TL0.075, we found similar results with GB being the most dynamic forefield with pixels that tended to become colonised by vegetation three years faster and with higher growth rates than average (Fig. 6A).

The two random forest models achieved an overall accuracy of 75% and 72% for TL and GR respectively, which translated a good capacity of the four predictors to classify time lag and growth rate anomalies as positive, negative, or absent. Mean decrease in accuracy (MDA) was used to order the four predictors according to their importance of overall classification accuracy (Fig. 7). SF-GDD was overall the most important predictor for both models (MDA = 0.128 [0.127] for TL [GR]) compared to Local vegetation, LS-factor, and Flow accumulation (respectively, 0.062 [0.052], 0.051 [0.041] and 0.044 [0.04] for TL [GR]). Overall, allogenic factors describing environmental context were more important than potential geomorphological disturbances variables (Fig. 7A and 7B). Classification probabilities showed that faster colonisation occurred with SF-GDD > 900 (Prob > 0.5) while slower colonisation occurred mostly between 500 and 900 SF-GDD. Slower growth rates occurred with SF-GDD > 500 while faster growth rate occurred sporadically above 900 SF-GDD (Fig. 7D). The class of undetected vegetation occurs mostly under 500 SF-GDD for both TL and GR (Fig. 7C and 7D).

#### 4.2. Agreement between field and Landsat observations of plant cover Floristic plots captures are representative of heterogeneity in glacier forefields vegetation dynamics heterogeneity

By comparing plant cover of the 297 floristic plots to the detection of vegetation as detected by Landsat NDVI, we found that the 221 floristic plots identified as unvegetated had an average plant cover of 5% (Fig. 6C). These results matched the initial sensitivity targeted considering the scale difference between Landsat pixel and floristic plots. Similarly, we found anomalies of TL0.075 and GR0.075 to be representative of the overall vegetation dynamics of glacier forefields as values tended to be similar when we compared only pixels that overlapped floristic plots to the entire forefield (Fig. 6A and 6B).

#### 4.3. Environmental context drives plant species assemblages and succession dynamics

The first axis of the NMDS showed a ~~thermal~~-floristic gradient representative of species turnover along an elevation gradient throughout the southwestern European Alps (Fig. 8A and 8B). Cold-adapted high alpine specialist species, ~~hereafter referred to as cold successional species~~, included ~~eds~~ low-stature, pioneer hemicryptophytes of sparsely vegetated screes, talus, and rock debris such as *Linaria alpina*, *Cerastium uniflorum* and *Saxifraga spp.* ~~More thermophilous~~ Species typically found at lower elevations, ~~hereafter referred to as warm successional species~~, included phanerophytes (*Picea abies*) and chamaephytes (*Vaccinium uliginosum*). Notably, ~~we observed early successional species this set of warm successional species as pioneer species~~ in the context of the Glacier Blanc, Pèlerins, and Tour glaciers, including trees and shrubs species such as *Larix decidua* and *Salix laggeri*.

The GLS model including a spatial correlation error structure had better fit (lower AICc) for the three allogenic variables and for flow accumulation. The importance of the spatial structure was particularly strong for elevation with a pseudo-R<sup>2</sup> of 0.74 without spatial autocorrelation to be compared to 0.23 with spatial autocorrelation. This indicated that the relationship between elevation and the floristic

composition was mainly driven by the elevational differences between glacier forefields. For all other variables, we found no major changes in the relationships between NMDS axes and variables. NMDS1 was positively-correlated to neighboring local-vegetation cover (pseudo  $R^2=0.6290$ ) and SF-GDD (pseudo  $R^2=0.5573987$ ) and negatively correlated to elevation ( $r^2=0.6747$ ) in the best fit models. NMDS1# was poorly correlated to other factors such as the LS factor ( $r^2=0.25624$ ), debris size ( $r^2=0.0836$ ), Flow accumulation ( $r^2=0.03497$ ) and time since deglaciation ( $r^2=0.0046$ ). By comparing NMDS1 scores to time since deglaciation, we found that elapsed time following deglaciation led to more late successional species for all glacier forefields (except PEL) but at a rate insufficient to surpass the effect of initial plant community composition (Fig. 9). We found that the initial starting point of the succession to be mostly driven by allogenic factors describing the environmental context (average  $r^2=0.68$ ), and not potential geomorphological disturbances (average  $r^2=0.1288$ ) or time available ( $r^2=0.0046$ ) (Table 1). Finally, we found that the heterogeneity of vegetation dynamics described through the anomalies of TL0.075 and GR0.075 were linked to the NMDS1 scores with slower colonisation (positive TL0.075 anomalies) and growth (negative GR0.075 anomalies) rate corresponding to lower NMDS1 site scores (Figure 10).

## 5. Discussion

Our comparative study of vegetation dynamics in glacier forefields based on two complementary and independent approaches provides insight into the heterogeneity of early plant succession dynamics after glacier retreat at the regional scale. First, using the Landsat time series, we found strong variability in the time lag between deglaciation and colonisation by plants and plant growth rate within and between glacier forefields (Fig. 4, 5 and 6). We showed that this heterogeneity was mostly explained by the local environmental context, i.e., local vegetation surrounding the forefields and energy availability linked to temperature and snowmelt gradients, rather than potential geomorphological context (Fig. 7). Similarly, by analysing turnover in plant species assemblages derived from field sampling, we found that the composition of early plant succession communities (0-35 years since deglaciation) established on glacier forefields, i.e., the initial starting point of plant succession, was highly variable from one glacier to another, and depended strongly on the topoclimatic context of the glacier forefield. Succession was also strongly correlated to allogenic factors describing the environmental context rather than potential geomorphological disturbances (Fig. 8 and Tab. 1). Interestingly, in most cases, we found that elapsed time since deglaciation was insufficient to overstep the determinism of the initial starting point, highlighting the importance of the local environmental context to understand early plant succession in glacier forefields (Fig. 9). Overall, both approaches converged towards this conclusion (Fig. 10) suggesting that early plant succession is not stochastic as previous authors have suggested (Wojcik et al., 2021) but rather deterministic in relation to environmental conditions.

### 5.1. Succession dynamics in glacier forefields are shaped by local environmental context

In our analysis, early vegetation dynamics in glacier forefields can be divided into two phases: (i) the lag between deglaciation and plant colonisation establishment (as detected by satellite); and (ii) the succession dynamics following initial plant colonisation establishment (Fig. 32). We analyzed the heterogeneity of the first phase through two approaches based on remote sensing. First, as we distinguished vegetated from non-vegetated pixels, we were able to estimate the proportion of glacier forefields to become colonized by vegetation with respect to time since deglaciation. We found strong heterogeneity between glacier forefields, with 80% of the forefield colonized by plants after 30 years for GB, TR, and STS, while the five other forefields did not reach 50% of vegetation cover over the same period, with no vegetation identified for LAU (Fig. 5). The second approach directly quantifies the time lag between deglaciation and plant colonisation establishment. Nonetheless, as the range of absolute time lag is constrained by the length of the period between the

year of deglaciation and the end of the time series, time lag could only be compared as anomalies regarding the median time lag for each year of deglaciation (Fig. 7A).

Time lag between deglaciation and plant establishment has been shown to be dependent on the proximity and availability of seed sources (Erschbamer et al., 2001, Stöcklin and Bäumler, 1996, Tackenberg and Stöcklin, 2008; Garbarino et al. 2010) and species ability to disperse (Fickert and Grüniger, 2018), findings which are consistent with our results. Indeed, using partial dependency analysis, we showed that the time lag anomalies (including the absence of vegetation detected) are distributed along the SF-GDD gradient, which in turn is highly correlated to both elevation and neighboring vegetation cover in the vicinity of local vegetation. [add that the relation remains while accounting for autocor spatial which strengthen the message] These results confirm that high elevation forefields surrounded by sparsely vegetated scree slopes in the immediate surroundings tend to be colonized more slowly than forefields at lower elevation with dense patches of vegetation nearby. This conclusion is supported if we consider the most and least dynamic forefields (in terms of vegetation colonization rate), respectively GB and LAU, which match these characteristics. In terms of spatial distribution, the GB forefield is also located at lower latitude and is the only south facing glacier forefield among the eight glaciers studied (Fig. 1), both of which contribute to earlier snowmelt-out and greater accumulation of growing degree days for an equivalent elevation located on a north-facing glacier situated at a higher latitude. Indeed, the left bank of the GB forefield has been described by Bayle (2020) as highly dynamic, which is confirmed here with colonization occurring within 1 to 5 years after deglaciation, as reported elsewhere in the European Alps (Burga et al., 2010, Cannone et al., 2007, Fickert and Grüniger, 2018). This specificity is known to be due to the proximity of a dense vegetation patch which was located at less than 100 m to the glacier tongue in 1984 and at low elevation (2400 m a.s.l.). Conversely, the LAU forefield deglaciated at the same period is located at 3100 m a.s.l., further to the north in the Grand Paradiso National Park with only sparse vegetation nearby (Mainetti et al., 2021).

While previous studies have reported consistent pioneer plant species and functional groups giving way to later successional species in the context of glacier forefields (e.g. Shumann et al. 2016), our study of multiple glacier forefields indicates that the identity of pioneer species varies highly from one site to another and depends strongly on local environmental context. Figure 9 shows that practically all of the plant communities encountered across the floristic gradient of the eight forefields have the potential to be pioneer species, given the wide range of initial starting points for initial community composition shown across NMDS scores. We emphasize that tree species such as Picea abies or Betula pubescens, or shrubs such as Salix laggeri, are just as capable of establishing quickly in the wake of glacier retreat as smaller stature forbs including Saxifraga or Poa spp. (Figure 8-9). Accordingly, we argue that the identity of pioneer species and the structure of community composition, as well as the subsequent rate of growth following establishment (Fig. 10), are strongly influenced during the first decades of succession by energy availability and nearby vegetation.

## 5.2. The importance of scale for geomorphological understanding drivers of plant succession dynamics

While we did not observe high explanatory power of geomorphic variables in explaining the heterogeneity of succession dynamics in glacier forefields, a large number of studies have shown otherwise (Gurnell et al., 2001, Moreau et al., 2008, Burga et al., 2010, Eichel et al., 2013, Temme and Lange, 2014, Klaar et al., 2015, Heckmann et al., 2016, Eichel et al., 2018, Eichel, 2019, Miller and Lane, 2018, Wojcik et al., 2020, Wojcik et al., 2021). Biogeomorphological studies emphasise that landscape dynamics within glacier forefields depend on the balance between stabilising and destructive forces (Eichel et al., 2018). Indeed, proglacial plant succession in the wake of deglaciation alters site conditions and decreases the magnitude and/or the spatial extent of geomorphological disturbances (Gurnell et al., 2000, Moreau et al., 2008, Eichel, 2019, Miller and Lane, 2018). More specifically, the biogeomorphic phase, characterized by feedbacks between abiotic and biotic processes, is a key stage of landscape stabilisation in glacier forefields. However, exacerbated fluvioglacial and hillslopes

Formatted: Indent: First line: 1.27 cm

Formatted: Font: 10 pt

processes within the deglaciated area during the first stage of the so-called paraglacial period may also delay the succession rate through rejuvenation of proglacial deposits (Wojcik et al., 2020).

Through the remote sensing and floristic approaches used here, GB displayed exceptionally fast colonisation in certain areas but also high heterogeneity within the forefield, with up to 30 years of difference in time lag for the same year of deglaciation (Fig. 6A). We attribute this heterogeneity to spatial variability in the intensity of potential geomorphological disturbance (Lardeux et al., 2015). Specifically, a gully area on the right bank of the forefield remains active and thus prevents vegetation establishment, as described by Bayle (2020) and Lardeux et al. (2015). This geomorphic activity is known to be the result of an active eroding slope supported by a slowly melting ice-cored moraine, which is a phenomenon too fine and complex to be captured by our low-resolution variables of potential instability. This example shows that, although the sum of degree days during the growing season (SF-GDD) and local vegetation explained most of the observed heterogeneity in observed vegetation dynamics (lag and growth rate), finer variables estimating direct instability and geomorphic activities based on a high-resolution imagery or field measures would locally change the balance of importance and improve the predictive capacity of models (Fig. 7). The PEL glacier provides a further example, where we observed long lag times and slow growth rates despite relatively low elevation and accordingly high SF-GDD, which we attribute to the extremely chaotic and blocky substrate observed in the field. Although we did attempt to capture potential geomorphological disturbances through substrate heterogeneity by calculating the weighted mean estimate of block size for floristic plots, we found similar results in this case compared to coarser DEM-based variables. Thus, we lacked a spatially continuous and ecologically relevant estimate of substrate properties. Estimating block size and geomorphological properties using a remote sensing approach has been explored (Westoby et al., 2017, Vázquez-Tarrio et al., 2017, Langhammer et al., 2019, Eichel et al., 2020, Lang et al., 2021) and constitutes an important perspective for enhancing the analysis conducted in the present study, perhaps especially in regard to later plant succession dynamics known to be particularly linked to bio-geomorphic feedbacks (Eichel et al., 2016, Miller and Lane, 2018, Lane et al., 2016).

We argue that the poor predictive capabilities of our geomorphological variables can be in part explained by the fact that those measures potential and not realised instability. Furthermore, the poor predictive capacity of our potential geomorphological disturbance variables could be explained by scale differences. Most studies highlighting the importance of geomorphic activities in explaining succession dynamics heterogeneity have been conducted at the glacier forefield scale at sub-meter spatial resolution. Our regional-scale approach showed that the local environmental context drives an initial starting point and that other local factors are insufficiently determinant to overrule it (Fig. 9A). We hypothesise that for our analysis, the importance of geomorphological variables and processes were overshadowed by broader-scale and more contextual drivers such as energy availability. Finally, because of the low sensitivity of our remote sensing approach (discriminating vegetation cover around 10% only), it is possible that we only detect vegetation that develops on stable surfaces unaffected by geomorphological activities. In other words, we might only detect vegetation after the battle between substrate instability and colonization by plants (Eichel et al. 2016), resulting in large underestimation of the importance of geomorphological activities.


### 5.3. The Landsat time series effectively captures vegetation dynamics in a real-time approach

The Landsat time series offers the possibility to study vegetation dynamics using a real-time approach, given its temporal resolution and depth (Wulder et al., 2019, Bayle et al., 2021). For the first time, we used the Landsat archive since the mid-1980s to quantify real-time plant colonization dynamics at the scale of glacier forefields, based on ecologically relevant indicators of time lag and growth rate following establishment. In the context of the observed generalized greening of the European Alps (Choler et al. 2021), these parameters provide

444 further insight into trajectories of plant colonization in the context of peri-glacial greening hotspots. Nonetheless, this approach inevitably  
445 comes with some uncertainty and bias that merit discussion.

446 Relationships between NDVI and certain biophysical properties of vegetation canopies, such as leaf area index (LAI), vegetation  
447 cover and biomass have been widely studied (Ormsby et al., 1987, Wittich and Hansing, 1995), including in the context of glacier forefields  
448 (Bayle et al., 2021, Knoflach et al., 2021) and in sparsely vegetated sites in the Antarctic (Fretwell et al., 2011). Further testing of relationships  
449 between NDVI and plant canopy properties in the context of glacier forefields remains necessary, however, to better understand the effects  
450 of specific conditions unrelated to vegetation that can alter reflectance, such as low organic content in soil (Todd et al., 1998), coarse  
451 granulometry and complex angular effects due to micro-topography (Bayle et al., 2021). Despite the difference in area between field plots  
452 (2x2m) and Landsat pixels (30x30m), we found similar sensitivity between ground truth vegetation cover and NDVI values to that of Bayle  
453 et al. (2021) and thus validate that within this study region an NDVI value of 0.075 efficiently identifies pixels with more of less than 5-  
454 10% of vegetation cover (Figure S10). Nonetheless, because of coarse resolution and noises inherent to NDVI time series, our approach is  
455 unable to detect reverse trends with vegetated pixels changing to unvegetated pixels. For example, after several years of vegetation detection,  
456 a sudden drop in NDVI resulting in the pixel being identified as unvegetated could be interpreted as the result of disturbance or due to  
457 spectral-related noises, with no possibilities to decipher one from another. Improvement of our approach could be done by using proper  
458 ground control information regarding abrupt disturbances in glacier forefields. Also, systematic UAV flight on each glacier forefield could  
459 drastically improve the calibration of satellite remote sensing methods while providing relevant information on vegetation distribution and  
460 geomorphic activities at one time (Woellner & Wagner, 2019; Healy & Khan, 2022; Lang et al. 2021; Westoby et al. 2017).

461 Finally Additionally, we found that to take full advantage of the time series, the presence of clouds was problematic as the actual  
462 cloud mask applied in the data distributed by the USGS (Fmask 3.3) is inefficient in high elevation areas as soil temperature is too low and  
463 is often confused with clouds (Qiu et al., 2017, Qiu et al., 2019b). Thus, we recommend using the modified MFmask 4.0 to improve the  
464 number of images available (Figure S8). Despite these challenges, our study thus confirms that the Landsat time series can be efficiently  
465 used to monitor vegetation cover changes over time in the context of glacier forefields.

466 

#### 467 5.4. Field sampling recommendations

469 Several studies have shown that the initial site conditions defined by substrate material, topography, micro-climate, landscape  
470 surroundings, as well as by varying ~~erratic~~ frequencies and/or magnitudes of natural disturbances between sites, are of high importance in  
471 determining plant succession dynamics in glacier forefields (Joly and Brossard, 2007, Walker and Wardle, 2014, Wojcik et al., 2020, Eichel  
472 et al., 2016). Repeated visits of permanent plots represent an alternative to the regular space-for-time approach as they provide a more  
473 informative and reliable measure of succession. This approach is costly in terms of effort, however, and furthermore it can be difficult to  
474 mark permanent plots in unstable terrain often found in glacier forefields (but see Bakker et al., 1996). An intermediate and less-costly  
475 approach consists in measuring variations in initial site conditions and geomorphological disturbances along the chronosequence, as proposed  
476 by Wojcik et al. (2021). In our field campaign, the eight glacier forefields were surveyed based on a random sampling approach along the  
477 chronosequence of deglaciation, however vegetation plots captured overall heterogeneity within forefields with varying degrees of success  
478 (Fig. 6). In accessible glacier forefields of small size and limited geomorphic activities (TR, PEL, GEB, STS and OR), our approach worked  
479 as floristic plots were found to be representative of the vegetation dynamics as assessed from the spatially exhaustive remote sensing  
480 approach (Fig. 6). The representativity was less evident for LAV, which can be explained by the large size of the forefield and the presence

Formatted: Font: 10 pt

Formatted: Indent: First line: 1.27 cm

of cliffs and a lake that drastically constrained accessibility. [Also, surfaces known to be affected by geomorphological activities might have been undersampled as for example the field sampling on GB forefield was mostly limited to the left bank as the right bank was too dangerous due to gullies and ice-cored moraines \(Lardeux et al. 2015; Bayle 2020\).](#) Noticeably, our results show that the within forefield variability in vegetation dynamics can be equivalent to the variability observed at regional scale, thus leading to massive bias in our capacity to extrapolate results when studies rely solely on a space-for-time approach applied to a single glacier forefield.

Our study provides lessons that could contribute toward improving future studies carried out in glacier forefields. Although explaining the absence of vegetation was not our question here, to understand where plants will establish, we recommend sampling points characterised by an absence of vegetation in addition to vegetated areas. Indeed, the first step in the primary succession dynamics is whether vegetation can colonise a surface. Thus, the absence of vegetation on deglaciated surfaces should be considered as an extreme case of equal ecological relevance as vegetated plots, especially in the context of biogeomorphic feedbacks and regular disturbances minimising the probability of establishment and germination. Thus, in the perspective of an exhaustive and representative sampling of the glacier forefield, collecting information on the absence of vegetation appears to be crucial for future field campaigns. Overall, we recommend the following procedure for future field campaigns:

- (1) Randomly select a predefined number of points using GIS software within targeted glacier forefields.
- (2) Collect information unrelated to vegetation on plots whether there is vegetation or not and keep track of unreachable random points due to dangerous access as it is a marker of high geomorphic activity, [and select plot size and location to facilitate alignment with satellite imagery.](#)
- (3) Measure plant community structure and composition, including functional traits, both within and outside of the glacier forefields to capture the local environmental context through field sampling.

## 6. Conclusion

We quantified heterogeneity in plant succession dynamics based on 36 years of optical satellite imagery and 297 floristic plots distributed among eight glacier forefields in the southwestern European Alps. The projection of autogenic and allogenic factors according to the definition presented in Wojcik et al. (2021) shows that the pioneer plant community composition is strongly correlated with environmental context rather than time since deglaciation. Time since deglaciation is typically identified as the main driver of succession dynamics, as it is fundamentally intrinsic to the idea of succession. Nonetheless, whether time since deglaciation is identified as the main driver of succession is a matter of scale. We showed that, indeed, if we consider each forefield independently, a clear successional gradient emerges as time since deglaciation increases. But when considering all eight glacier forefields together, energy availability and initial species composition emerged as the key parameters shaping successional dynamics. In the case of both remotely sensed vegetation indices and plant field surveys, we found that this initial starting point was strongly correlated to the local environmental context, rather than the geomorphological context, [suggesting that the notion of a “pioneer” species is actually quite flexible](#) (Table 1). Overall, our findings suggest that early stages of plant succession in glacier forefields in the European Alps are highly dependent on the local environmental context and less stochastic than previous studies have suggested.

In the conceptual framework of Wojcik et al. (2021), our findings suggest a reinterpretation of the importance of local environmental context in the initial stages of primary succession, which is considered to be highly stochastic (Chase and Myers, 2011, Dini-Andreote et al., 2015, del Moral, 2009, Mong and Vetaas, 2006, Marteinsdóttir et al., 2010). In contrast, we found that this initial phase was driven by plant opportunism originating from [neighboring vegetationthe local species pool](#), which is a function of environmental context

and other biogeographic factors. We highlighted that ~~forduring the first 30 years of succession, initial plant community composition was far more important than time since deglaciation in shaping plant assemblages and rates of colonization, time since deglaciation became a meaningless predictor of plant community composition when multiple and highly contrasting glacier forefields were considered,~~ thus pointing to the importance of quantifying more direct drivers of succession dynamics including both environmental and biological factors. Our work highlights the ongoing need for process-based studies combining remote sensing and field techniques to improve our understanding of local heterogeneity in plant colonisation trajectories, and furthermore provides a promising basis for predicting future trajectories of plant succession in the wake of ongoing glacier retreat during the coming decades using widely available remotely sensed predictors.

**Data availability**

Research data can be accessed upon request to the corresponding author. Part of the data used in this paper remains under exclusivity as it was obtained through multiple programs and partnerships.

**Author contribution**

**Conceptualisation** AB and BC **Data curation** All authors contributed **Formal analysis** AB and BC **Writing – Original draft and preparation** AB and BC **Writing – review and editing** All authors contributed

**Competing interests**

The authors declare no competing interests.

**References**

Anthelme, F., Cauvy-Fraunié, S., Francou, B., Cáceres, B. & Dangles, O. 2021. Living at the Edge: Increasing Stress for Plants 2–13 Years After the Retreat of a Tropical Glacier. *Frontiers in Ecology and Evolution*, 9.

Bakker, J. P., Poschlod, P., Strykstra, R. J., Bekker, R. M. & Thompson, K. 1996. Seed banks and seed dispersal: important topics in restoration ecology. *Acta Botanica Neerlandica*, 45, 461–490.

Barrou Dumont, Z., Gascoin, S., Hagolle, O., Ablain, M., Jugier, R., Salgues, G., Marti, F., Dupuis, A., Dumont, M. & Morin, S. 2021. Brief communication: Evaluation of the snow cover detection in the Copernicus High Resolution Snow & Ice Monitoring Service. *The Cryosphere*, 15, 4975–4980.

Bayle, A. 2020. A recent history of deglaciation and vegetation establishment in a contrasted geomorphological context, Glacier Blanc, French Alps. *Journal of Maps*, 16, 766–775.

Bayle, A., Roussel, E., Carlson, B. Z., Vautier, F., Brossard, C., Fovet, E., De Bouchard D’aubeterre, G. & Corenblit, D. 2021. Sensitivity of Landsat NDVI to subpixel vegetation and topographic components in glacier forefields: assessment from high-resolution multispectral UAV imagery. *Journal of Applied Remote Sensing*, 15.

Bayle, A., Roy, A., Dedieu, J.-P., Boudreau, S., Choler, P. & Lévesque, E. 2022. Two distinct waves of greening in northeastern Canada: summer warming does not tell the whole story. *Environmental Research Letters*, 17, 064051.

Barton, K. 2023. MuMIn: Multi-Model Inference. R package version 1.47.2/r505, <https://R-Forge.R-project.org/projects/mumin/>.

Bradshaw, A. D. 1993. Restoration Ecology as a Science. *Restoration Ecology*, 1, 71–73.

Breen, K. & Lévesque, E. 2008. The Influence of Biological Soil Crusts on Soil Characteristics along a High Arctic Glacier Foreland, Nunavut, Canada. *Arctic, Antarctic, and Alpine Research*, 40, 287–297.

Breiman, L. 2001. <Breiman2001\_Article\_RandomForests.pdf>. *Machine Learning*, 45, 5–32.

Burga, C. A., Krüsi, B., Egli, M., Wernli, M., Elsener, S., Zieffle, M., Fischer, T. & Mavris, C. 2010. Plant succession and soil development on the foreland of the Morteratsch glacier (Pontresina, Switzerland): Straight forward or chaotic? *Flora - Morphology, Distribution, Functional Ecology of Plants*, 205, 561–576.

- Cannone, N., Sgorbati, S. & Guglielmin, M. 2007. Unexpected impacts of climate change on alpine vegetation. *Frontiers in Ecology and the Environment*, 5, 360-364.
- Carlson, B. Z., Choler, P., Renaud, J., Dedieu, J. P. & Thuiller, W. 2015. Modelling snow cover duration improves predictions of functional and taxonomic diversity for alpine plant communities. *Annals of Botany*, 116, 1023-34.
- Carlson, B. Z., Corona, M. C., Dentant, C., Bonet, R., Thuiller, W. & Choler, P. 2017. Observed long-term greening of alpine vegetation—a case study in the French Alps. *Environmental Research Letters*, 12, 114006.
- Cauvy-Fraunie, S. & Dangles, O. 2019. A global synthesis of biodiversity responses to glacier retreat. *Nat Ecol Evol*, 3, 1675-1685.
- Chapin, F. S., Walker, L. R., Fastie, C. L. & Sharman, L. C. 1994. Mechanisms of Primary Succession Following Deglaciation at Glacier Bay, Alaska. *Ecological Monographs*, 64, 149-175.
- Chase, J. M. & Myers, J. A. 2011. Disentangling the importance of ecological niches from stochastic processes across scales. *Philosophical Transactions of the Royal Society of London B Biological Sciences*, 366, 2351-63.
- Choler, P. 2005. Consistent Shifts in Alpine Plant Traits along a Mesotopographical Gradient. *Arctic, Antarctic, and Alpine Research*, 37, 444-453.
- Choler, P. 2015. Growth response of temperate mountain grasslands to inter-annual variations in snow cover duration. *Biogeosciences*, 12, 3885-3897.
- Choler, P. 2018. Winter soil temperature dependence of alpine plant distribution: Implications for anticipating vegetation changes under a warming climate. *Perspectives in Plant Ecology, Evolution and Systematics*, 30, 6-15.
- Choler, P., Bayle, A., Carlson, B. Z., Randin, C., Filippa, G. & Cremonese, E. 2021. The tempo of greening in the European Alps: Spatial variations on a common theme. *Global Change Biology*, 27, 5614-5628.
- Conrad, O., Bechtel, B., Bock, M., Dietrich, H., Fischer, E., Gerlitz, L., Wehberg, J., Wichmann, V. & Böhner, J. 2015. System for Automated Geoscientific Analyses (SAGA) v. 2.1.4. *Geoscientific Model Development*, 8, 1991-2007.
- Del Moral, R. 2009. Increasing deterministic control of primary succession on Mount St. Helens, Washington. *Journal of Vegetation Science*, 20, 1145-1154.
- Desmet, P. J. J. & Govers, G. 1996. A GIS procedure for automatically calculating the USLE LS factor on topographically complex landscape units. *Journal of Soil and Water Conservation*, 51.
- Dini-Andreote, F., Stegen, J. C., Van Elsas, J. D. & Salles, J. F. 2015. Disentangling mechanisms that mediate the balance between stochastic and deterministic processes in microbial succession. *Proceedings of the National Academy of Sciences of the United States of America*, 112, E1326-32.
- Eastman, J., Sangermano, F., Ghimire, B., Zhu, H., Chen, H., Neeti, N., Cai, Y., Machado, E. A. & Crema, S. C. 2009. Seasonal trend analysis of image time series. *International Journal of Remote Sensing*, 30, 2721-2726.
- Eichel, J. 2019. Vegetation Succession and Biogeomorphic Interactions in Glacier Forelands. 327-349.
- Eichel, J., Corenblit, D. & Dikau, R. 2016. Conditions for feedbacks between geomorphic and vegetation dynamics on lateral moraine slopes: a biogeomorphic feedback window. *Earth Surface Processes and Landforms*, 41, 406-419.
- Eichel, J., Draebing, D., Kattenborn, T., Senn, J. A., Klingbeil, L., Wieland, M. & Heinz, E. 2020. Unmanned aerial vehicle-based mapping of turf-banked solifluction lobe movement and its relation to material, geomorphometric, thermal and vegetation properties. *Permafrost and Periglacial Processes*, 31, 97-109.
- Eichel, J., Draebing, D. & Meyer, N. 2018. From active to stable: Paraglacial transition of Alpine lateral moraine slopes. *Land Degradation & Development*, 29, 4158-4172.
- Eichel, J., Krautblatter, M., Schmidtlein, S. & Dikau, R. 2013. Biogeomorphic interactions in the Turtmann glacier forefield, Switzerland. *Geomorphology*, 201, 98-110.
- Erschbamer, B., Kneringer, E. & Schlag, R. N. 2001. Seed rain, soil seed bank, seedling recruitment, and survival of seedlings on a glacier foreland in the Central Alps. *Flora*, 196, 304-312.
- Ficetola, G. F., Marta, S., Guerrieri, A., Gobbi, M., Ambrosini, R., Fontaneto, D., Zerboni, A., Poulenard, J., Caccianiga, M. & Thuiller, W. 2021. Dynamics of Ecological Communities Following Current Retreat of Glaciers. *Annual Review of Ecology, Evolution, and Systematics*, 52, 405-426.
- Fickert, T. & Grüniger, F. 2018. High-speed colonization of bare ground-Permanent plot studies on primary succession of plants in recently deglaciated glacier forelands. *Land Degradation & Development*, 29, 2668-2680.
- Fischer, A., Fickert, T., Schwaizer, G., Patzelt, G. & Gross, G. 2019. Vegetation dynamics in Alpine glacier forelands tackled from space. *Scientific Reports*, 9, 13918.
- Franzén, M., Dieker, P., Schrader, J. & Helm, A. 2019. Rapid plant colonization of the forelands of a vanishing glacier is strongly associated with species traits. *Arctic, Antarctic, and Alpine Research*, 51, 366-378.
- Fretwell, P. T., Convey, P., Fleming, A. H., Peat, H. J. & Hughes, K. A. 2011. Detecting and mapping vegetation distribution on the Antarctic Peninsula from remote sensing data. *Polar Biology*, 34, 273-281.
- Garbarino, M., Lingua, E., Nagel, T. A., Godone, D., Motta, R. 2010. Patterns of larch establishment following deglaciation of Ventina glacier, central Italian Alps. *Forest Ecology and Management*, 259 (3), 583-590.



- Gardent, M., Rabatel, A., Dedieu, J.-P. & Deline, P. 2014. Multitemporal glacier inventory of the French Alps from the late 1960s to the late 2000s. *Global and Planetary Change*, 120, 24-37.
- Garibotti, I. A., Pissolito, C. I. & Villalba, R. 2011. Spatiotemporal Pattern of Primary Succession in Relation to Meso-topographic Gradients on Recently Deglaciated Terrains in the Patagonian Andes. *Arctic, Antarctic, and Alpine Research*, 43, 555-567.
- Gascoin, S., Grizonnet, M., Bouchet, M., Salgues, G. & Hagolle, O. 2019. Theia Snow collection: high-resolution operational snow cover maps from Sentinel-2 and Landsat-8 data. *Earth System Science Data*, 11, 493-514.
- Gobiet, A., Kotlarski, S., Beniston, M., Heinrich, G., Rajczak, J. & Stoffel, M. 2014. 21st century climate change in the European Alps--a review. *Science of the Total Environment*, 493, 1138-51.
- Górnaiak, D., Marszałek, H., Kwaśniak-Kominek, M., Rzepa, G. & Manecki, M. 2017. Soil formation and initial microbiological activity on a foreland of an Arctic glacier (SW Svalbard). *Applied Soil Ecology*, 114, 34-44.
- Greenwell, B. M. 2017. pdp: An R Package for Constructing Partial Dependence Plots. *The R Journal*, 9, 421.
- Gurnell, A. M., Edwards, P. J., Petts, G. E. & Ward, J. V. 2000. A conceptual model for alpine proglacial river channel evolution under changing climatic conditions. *Catena*, 38, 223-242.
- Gurnell, A. M., Petts, G. E., Hannah, D. M., Smith, B. P. G., Edwards, P. J., Kollmann, J., Ward, J. V. & Tockner, K. 2001. Riparian vegetation and island formation along the gravel-bed Fiume Tagliamento, Italy. *Earth Surface Processes and Landforms*, 26, 31-62.
- Haerberli, W., Schaub, Y. & Huggel, C. 2017. Increasing risks related to landslides from degrading permafrost into new lakes in de-glaciating mountain ranges. *Geomorphology*, 293, 405-417.
- Healy, S. M., Khan, A. L. 2022. Mapping glacier ablation with a UAV in the North Cascades: A structure-from-motion approach. *Frontiers in Remote Sensing*, 57.
- Heckmann, T., Mccoll, S. & Morche, D. 2016. Retreating ice: research in pro-glacial areas matters. *Earth Surface Processes and Landforms*, 41, 271-276.
- Huss, M., Bookhagen, B., Huggel, C., Jacobsen, D., Bradley, R. S., Clague, J. J., Vuille, M., Buytaert, W., Cayan, D. R., Greenwood, G., Mark, B. G., Milner, A. M., Weingartner, R. & Winder, M. 2017. Toward mountains without permanent snow and ice. *Earth's Future*, 5, 418-435.
- Hutchinson, M. F., Xu, T. & Stein, J. A. 2011. Recent progress in the ANUDEM elevation gridding procedure. *Geomorphometry*.
- Johnson, E. A. & Miyanishi, K. 2008. Testing the assumptions of chronosequences in succession. *Ecology Letters*, 11, 419-31.
- Joly, D. & Brossard, T. 2007. Contribution of environmental factors to temperature distribution at different resolution levels on the forefield of the Loven Glaciers, Svalbard. *Polar Record*, 43, 353-359.
- Khedim, N., Cecillon, L., Poulenard, J., Barre, P., Baudin, F., Marta, S., Rabatel, A., Dentant, C., Cauvy-Fraunie, S., Anthelme, F., Gielly, L., Ambrosini, R., Franzetti, A., Azzoni, R. S., Caccianiga, M. S., Compostella, C., Clague, J., Tielidze, L., Messenger, E., Choler, P. & Ficetola, G. F. 2021. Topsoil organic matter build-up in glacier forelands around the world. *Global Change Biology*, 27, 1662-1677.
- Klaar, M. J., Kidd, C., Malone, E., Bartlett, R., Pinay, G., Chapin, F. S. & Milner, A. 2015. Vegetation succession in deglaciated landscapes: implications for sediment and landscape stability. *Earth Surface Processes and Landforms*, 40, 1088-1100.
- Knoflach, B., Ramskogler, K., Talluto, M., Hofmeister, F., Haas, F., Heckmann, T., Pfeiffer, M., Piermattei, L., Ressler, C., Wimmer, M. H., Geitner, C., Erschbamer, B. & Stötter, J. 2021. Modelling of Vegetation Dynamics from Satellite Time Series to Determine Proglacial Primary Succession in the Course of Global Warming—A Case Study in the Upper Martell Valley (Eastern Italian Alps). *Remote Sensing*, 13, 4450.
- Lane, S. N., Borgeaud, L. & Vittoz, P. 2016. Emergent geomorphic-vegetation interactions on a subalpine alluvial fan. *Earth Surface Processes and Landforms*, 41, 72-86.
- Lang, N., Imiger, A., Rozniak, A., Hunziker, R., Wegner, J. D. & Schindler, K. 2021. GRAINet: mapping grain size distributions in river beds from UAV images with convolutional neural networks. *Hydrology and Earth System Sciences*, 25, 2567-2597.
- Langhammer, L., Grab, M., Bauder, A. & Maurer, H. 2019. Glacier thickness estimations of alpine glaciers using data and modeling constraints. *The Cryosphere*, 13, 2189-2202.
- Lardeux, P., Glasser, N., Holt, T. & Hubbard, B. 2015. Glaciological and geomorphological map of Glacier Noir and Glacier Blanc, French Alps. *Journal of Maps*, 12, 582-596.
- Legendre, P. & Gallagher, E. D. 2001. Ecologically meaningful transformations for ordination of species data. *Oecologia*, 129, 271-280.
- Liaw, A. & Wiener, M. 2002. Classification and regression by randomForest. *R News*, 2/3.
- Linsbauer, A., Huss, M., Hodel, E., Bauder, A., Fischer, M., Weidmann, Y., Bärtschi, H. & Schmassmann, E. 2021. The New Swiss Glacier Inventory SGI2016: From a Topographical to a Glaciological Dataset. *Frontiers in Earth Science*, 9.
- Mainetti, A., D'amico, M., Probo, M., Quaglia, E., Ravetto Enri, S., Celi, L. & Lonati, M. 2021. Successional Herbaceous Species Affect Soil Processes in a High-Elevation Alpine Proglacial Chronosequence. *Frontiers in Environmental Science*, 8.
- Markham, B. L. & Helder, D. L. 2012. Forty-year calibrated record of earth-reflected radiance from Landsat: A review. *Remote Sensing of Environment*, 122, 30-40.

Formatted: Font colour: Auto

- Marta, S., Azzoni, R. S., Fugazza, D., Tielidze, L., Chand, P., Sieron, K., Almond, P., Ambrosini, R., Anthelme, F., Alviz Gazitúa, P., Bhambri, R., Bonin, A., Caccianiga, M., Cauvy-Fraunié, S., Ceballos Lievano, J. L., Clague, J., Cochachín Rapre, J. A., Dangles, O., Deline, P., Eger, A., Cruz Encarnación, R., Erokhin, S., Franzetti, A., Gielly, L., Gili, F., Gobbi, M., Guerrieri, A., Hågvær, S., Khedim, N., Kinyanjui, R., Messager, E., Morales-Martínez, M. A., Peyre, G., Pittino, F., Poulenard, J., Seppi, R., Chand Sharma, M., Urseitova, N., Weissling, B., Yang, Y., Zaginaev, V., Zimmer, A., Diolaiuti, G. A., Rabatel, A. & Fietola, G. F. 2021. The Retreat of Mountain Glaciers since the Little Ice Age: A Spatially Explicit Database. *Data*, 6, 107.
- Marteinsdóttir, B., Svavarsdóttir, K. & Thórhallsdóttir, T. E. 2010. Development of vegetation patterns in early primary succession. *Journal of Vegetation Science*, 21, 531-540.
- Martín-Ortega, P., García-Montero, L. G. & Sibelet, N. 2020. Temporal Patterns in Illumination Conditions and Its Effect on Vegetation Indices Using Landsat on Google Earth Engine. *Remote Sensing*, 12, 211.
- Masek, J. G., Vermote, E. F., Saleous, N. E., Wolfe, R., Hall, F. G., Huemmrich, K. F., Gao, F., Kutler, J. & Lim, T. K. 2006. A Landsat Surface Reflectance Dataset for North America, 1990–2000. *IEEE Geoscience and Remote Sensing Letters*, 3, 68-72.
- Matthews, J. A. & Briffa, K. R. 2005. The 'little ice age': re-evaluation of an evolving concept. *Geografiska Annaler: Series A, Physical Geography*, 87, 17-36.
- Miller, H. R. & Lane, S. N. 2018. Biogeomorphic feedbacks and the ecosystem engineering of recently deglaciated terrain. *Progress in Physical Geography: Earth and Environment*, 43, 24-45.
- Minchin, P. R. 1987. An evaluation of the relative robustness of techniques for ecological ordination. *Vegetatio*, 69, 89-107.
- Mong, C. E. & Vetaas, O. R. 2006. Establishment of Pinus Wallichiana on a Himalayan Glacier Foreland: Stochastic Distribution or Safe Sites? *Arctic, Antarctic, and Alpine Research*, 38, 584-592.
- Moreau, M., Mercier, D., Laffly, D. & Roussel, E. 2008. Impacts of recent paraglacial dynamics on plant colonization: A case study on Midtre Lovénbreen foreland, Spitsbergen (79°N). *Geomorphology*, 95, 48-60.
- Nagol, J. R., Sexton, J. O., Kim, D.-H., Anand, A., Morton, D., Vermote, E. & Townshend, J. R. 2015. Bidirectional effects in Landsat reflectance estimates: Is there a problem to solve? *ISPRS Journal of Photogrammetry and Remote Sensing*, 103, 129-135.
- Oksanen, J., Blanchet, F. G., Friendly, M., Kindt, R., Legendre, P., Mcglinn, D., Minchin, P. R., O'hara, R. B., Simpson, G. L., Solymos, P., Henry, M., H. Stevens, Szoecs, E. & Wagner, H. 2020. vegan: Community Ecology Package.
- Ormsby, J. P., Choudhury, B. J. & Owe, M. 1987. Vegetation spatial variability and its effect on vegetation indices. *International Journal of Remote Sensing*, 8, 1301-1306.
- Painter, T. H., Flanner, M. G., Kaser, G., Marzeion, B., Vancuren, R. A. & Abdalati, W. 2013. End of the Little Ice Age in the Alps forced by industrial black carbon. *Proceedings of the National Academy of Sciences of the United States of America*, 110, 15216-21.
- Pickett, S. T. A. 1989. Space-for-Time Substitution as an Alternative to Long-Term Studies. 110-135.
- Pinheiro, J., Bates, D., R Core Team 2022. nlme: Linear and Nonlinear Mixed Effects Models R package version 3.1-160 <https://CRAN.R-project.org/package=nlme>
- Qiu, S., He, B., Zhu, Z., Liao, Z. & Quan, X. 2017. Improving Fmask cloud and cloud shadow detection in mountainous area for Landsats 4–8 images. *Remote Sensing of Environment*, 199, 107-119.
- Qiu, S., Lin, Y., Shang, R., Zhang, J., Ma, L. & Zhu, Z. 2019a. Making Landsat Time Series Consistent: Evaluating and Improving Landsat Analysis Ready Data. *Remote Sensing*, 11, 51.
- Qiu, S., Zhu, Z. & He, B. 2019b. Fmask 4.0: Improved cloud and cloud shadow detection in Landsats 4–8 and Sentinel-2 imagery. *Remote Sensing of Environment*, 231, 111205.
- Raffl, C., Mallaun, M., Mayer, R. & Erschbamer, B. 2006. Vegetation Succession Pattern and Diversity Changes in a Glacier Valley, Central Alps, Austria. *Arctic, Antarctic, and Alpine Research*, 38, 421-428.
- Robbins, J. A. & Matthews, J. A. 2010. Regional Variation in Successional Trajectories and Rates of Vegetation Change on Glacier Forelands in South-Central Norway. *Arctic, Antarctic, and Alpine Research*, 42, 351-361.
- Robbins, J. A. & Matthews, J. A. 2014. Use of ecological indicator values to investigate successional change in boreal to high-alpine glacier-foreland chronosequences, southern Norway. *The Holocene*, 24, 1453-1464.
- Rosero, P., Crespo-Pérez, V., Espinosa, R., Andino, P., Barragán, A., Moret, P., Gobbi, M., Fietola, G. F., Jaramillo, R., Muriel, P., Anthelme, F., Jacobsen, D., Dangles, O., Condom, T., Gielly, L., Poulenard, J., Rabatel, A., Basantes, R., Cáceres Correa, B. & Cauvy-Fraunié, S. 2021. Multi-taxa colonisation along the foreland of a vanishing equatorial glacier. *Ecography*, 44, 1010-1021.
- Roy, D. P., Kovalskyy, V., Zhang, H. K., Vermote, E. F., Yan, L., Kumar, S. S. & Egorov, A. 2016a. Characterization of Landsat-7 to Landsat-8 reflective wavelength and normalized difference vegetation index continuity. *Remote Sensing of Environment*, 185, 57-70.
- Roy, D. P., Zhang, H. K., Ju, J., Gomez-Dans, J. L., Lewis, P. E., Schaaf, C. B., Sun, Q., Li, J., Huang, H. & Kovalskyy, V. 2016b. A general method to normalize Landsat reflectance data to nadir BRDF adjusted reflectance. *Remote Sensing of Environment*, 176, 255-271.
- Rydgren, K., Halvorsen, R., Töpper, J. P., Njøs, J. M. & Del Moral, R. 2014. Glacier foreland succession and the fading effect of terrain age. *Journal of Vegetation Science*, 25, 1367-1380.

- Schaaf, C. B., Gao, F., Strahler, A. H., Lucht, W., Li, X., Tsang, T., Strugnell, N. C., Zhang, X., Jin, Y., Muller, J.-P., Lewis, P., Barnsley, M., Hobson, P., Disney, M., Roberts, G., Dunderdale, M., Doll, C., D'entremont, R. P., Hu, B., Liang, S., Privette, J. L. & Roy, D. 2002. First operational BRDF, albedo nadir reflectance products from MODIS. *Remote Sensing of Environment*, 83, 135-148.
- Scherrer, D. & Körner, C. 2011. Topographically controlled thermal-habitat differentiation buffers alpine plant diversity against climate warming. *Journal of Biogeography*, 38, 406-416.
- Schumann, K., Gewolf, S. & Tackenberg, O. 2016. Factors affecting primary succession of glacier foreland vegetation in the European Alps. *Alpine Botany*, 126, 105-117.
- Sigl, M., Abram, N. J., Gabrieli, J., Jenk, T. M., Osmont, D. & Schwikowski, M. 2018. 19th century glacier retreat in the Alps preceded the emergence of industrial black carbon deposition on high-alpine glaciers. *The Cryosphere*, 12, 3311-3331.
- Soenen, S. A., Peddle, D. R. & Coburn, C. A. 2005. SCS+C: a modified Sun-canopy-sensor topographic correction in forested terrain. *IEEE Transactions on Geoscience and Remote Sensing*, 43, 2148-2159.
- Sola, I., González-Audicana, M. & Álvarez-Mozos, J. 2016. Multi-criteria evaluation of topographic correction methods. *Remote Sensing of Environment*, 184, 247-262.
- Steven, M. D., Malthus, T. J., Baret, F., Xu, H. & Chopping, M. J. 2003. Intercalibration of vegetation indices from different sensor systems. *Remote Sensing of Environment*, 88, 412-422.
- Stöcklin, J. & Bäumler, E. 1996. Seed rain, seedling establishment and clonal growth strategies on a glacier foreland. *Journal of Vegetation Science*, 7, 45-56.
- Tackenberg, O. & Stöcklin, J. 2008. Wind dispersal of alpine plant species: A comparison with lowland species. *Journal of Vegetation Science*, 19, 109-118.
- Temme, A. J. a. M. & Lange, K. 2014. Pro-glacial soil variability and geomorphic activity - the case of three Swiss valleys. *Earth Surface Processes and Landforms*, n/a-n/a.
- Todd, S. W., Hoffer, R. M. & Milchunas, D. G. 1998. Biomass estimation on grazed and ungrazed rangelands using spectral indices. *International Journal of Remote Sensing*, 19, 427-438.
- Tucker, C. J. & Sellers, P. J. 1986. Satellite remote sensing of primary production. *International Journal of Remote Sensing*, 7, 1395-1416.
- Vázquez-Tarrio, D., Borgniet, L., Liébault, F. & Recking, A. 2017. Using UAS optical imagery and SfM photogrammetry to characterize the surface grain size of gravel bars in a braided river (Vénéon River, French Alps). *Geomorphology*, 285, 94-105.
- Vernay, M., Lafayasse, M., Monteiro, D., Hagenmuller, P., Nheili, R., Samacoits, R., Verfaillie, D. & Morin, S. 2022. The S2M meteorological and snow cover reanalysis over the French mountainous areas: description and evaluation (1958–2021). *Earth System Science Data*, 14, 1707-1733.
- Vincent, C., Harter, M., Gilbert, A., Berthier, E. & Six, D. 2014. Future fluctuations of Mer de Glace, French Alps, assessed using a parameterized model calibrated with past thickness changes. *Annals of Glaciology*, 55, 15-24.
- Vincent, C., Le Meur, E., Six, D. & Funk, M. 2005. Solving the paradox of the end of the Little Ice Age in the Alps. *Geophysical Research Letters*, 32.
- Walker, L. R. & Wardle, D. A. 2014. Plant succession as an integrator of contrasting ecological time scales. *Trends in Ecology & Evolution*, 29, 504-10.
- Westoby, M. J., Dunning, S. A., Woodward, J., Hein, A. S., Marrero, S. M., Winter, K. & Sugden, D. E. 2017. Sedimentological characterization of Antarctic moraines using UAVs and Structure-from-Motion photogrammetry. *Journal of Glaciology*, 61, 1088-1102.
- Wittich, K.-P. & Hansing, O. 1995. Area-averaged vegetative cover fraction estimated from satellite data. *International Journal of Biometeorology*, 38, 209-215.
- Wojcik, R., Donhauser, J., Frey, B. & Benning, L. G. 2020. Time since deglaciation and geomorphological disturbances determine the patterns of geochemical, mineralogical and microbial successions in an Icelandic foreland. *Geoderma*, 379, 114578.
- Wojcik, R., Eichel, J., Bradley, J. A. & Benning, L. G. 2021. How allogenic factors affect succession in glacier forefields. *Earth-Science Reviews*, 218, 103642.
- Woellner, R., Wagner, T. C. 2019. Saving species, time and money: Application of unmanned aerial vehicles (UAVs) for monitoring of an endangered alpine river specialist in a small nature reserve. *Biological conservation*, 233, 162-175.
- Wulder, M. A., Loveland, T. R., Roy, D. P., Crawford, C. J., Masek, J. G., Woodcock, C. E., Allen, R. G., Anderson, M. C., Belward, A. S., Cohen, W. B., Dwyer, J., Erb, A., Gao, F., Griffiths, P., Helder, D., Hermosilla, T., Hipple, J. D., Hostert, P., Hughes, M. J., Huntington, J., Johnson, D. M., Kennedy, R., Kilic, A., Li, Z., Lymburner, L., Mccorkel, J., Pahlevan, N., Scambos, T. A., Schaaf, C., Schott, J. R., Sheng, Y., Storey, J., Vermote, E., Vogelmann, J., White, J. C., Wynne, R. H. & Zhu, Z. 2019. Current status of Landsat program, science, and applications. *Remote Sensing of Environment*, 225, 127-147.
- Zhang, H. K., Roy, D. P. & Kovalsky, V. 2016. Optimal Solar Geometry Definition for Global Long-Term Landsat Time-Series Bidirectional Reflectance Normalization. *IEEE Transactions on Geoscience and Remote Sensing*, 54, 1410-1418.
- Zhu, Z. & Woodcock, C. E. 2012. Object-based cloud and cloud shadow detection in Landsat imagery. *Remote Sensing of Environment*, 118, 83-94.

Formatted: Font colour: Auto

781 Zhu, Z. & Woodcock, C. E. 2014. Automated cloud, cloud shadow, and snow detection in multitemporal Landsat data: An algorithm designed  
782 specifically for monitoring land cover change. *Remote Sensing of Environment*, 152, 217-234.  
783 Zimmer, A., Meneses, R. I., Rabatel, A., Soruco, A., Dangles, O. & Anthelme, F. 2018. Time lag between glacial retreat and upward  
784 migration alters tropical alpine communities. *Perspectives in Plant Ecology, Evolution and Systematics*, 30, 89-102.

785  
786  
787  
788  
789  
790  
791  
792  
793  
794  
795  
796  
797  
798  
799  
800  
801  
802  
803  
804  
805  
806  
807  
808  
809  
810  
811  
812

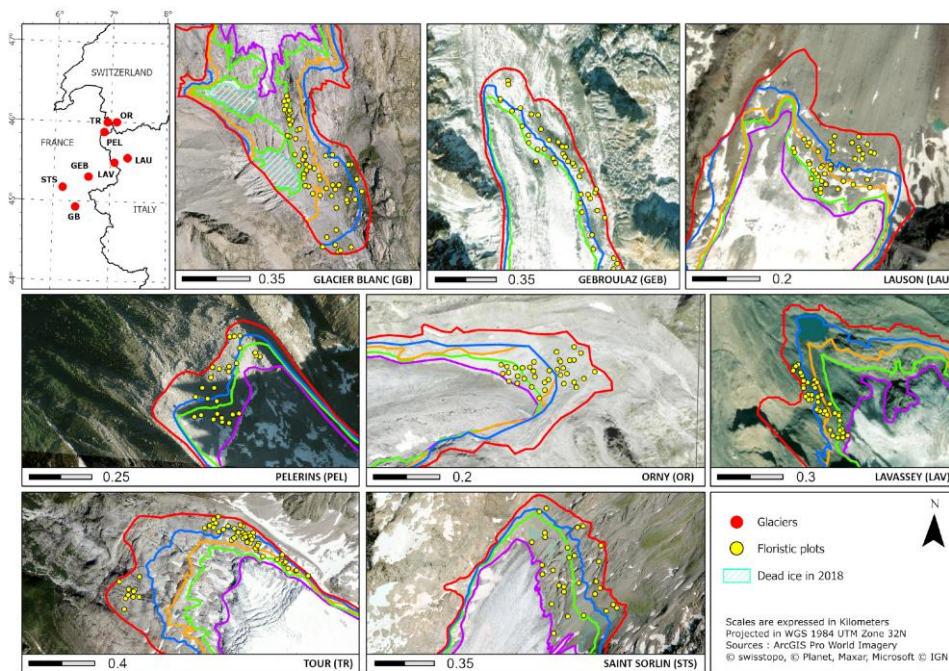


**Figure 1.** Distribution of the eight glacier margins in France, Switzerland, and Italy with corresponding abbreviations. Floristic plots are indicated in yellow points while glacier outlines are shown in thick coloured lines. Colours do not indicate similar outlines date but chronosequence of deglaciation. Corresponding years of deglaciation is to be found in Table S1. Projection and sources details are indicated in the bottom right panel.

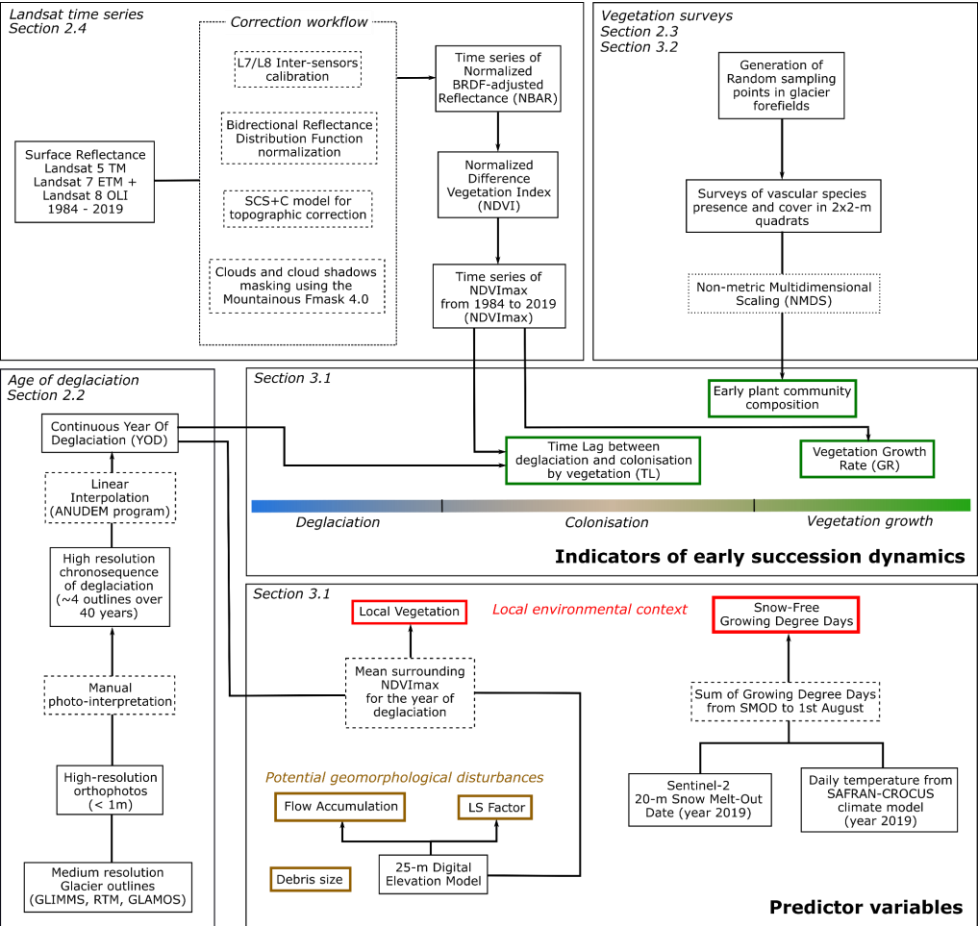


**Figure 2.** Complete analysis workflow shown by methodological sections. Indicators of early succession dynamics are shown in green while predictor variables are shown in red and brown.

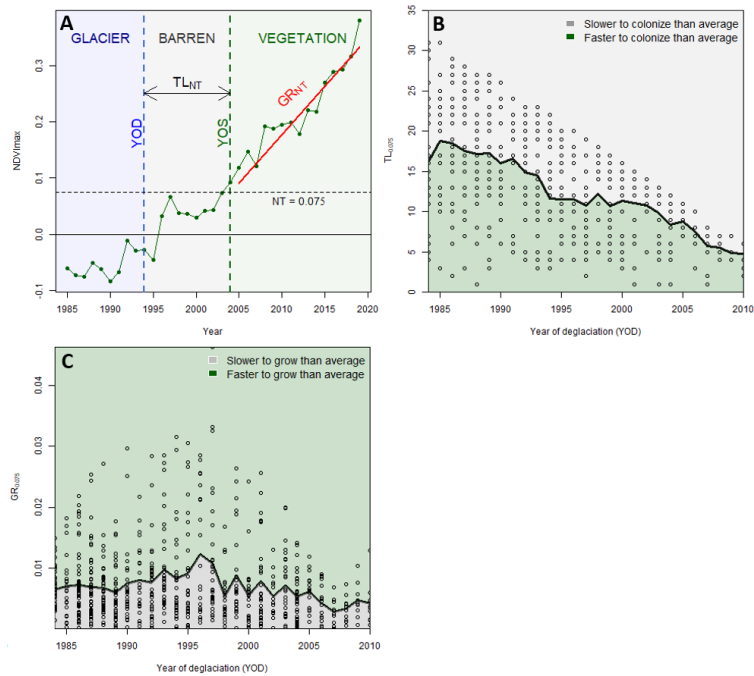
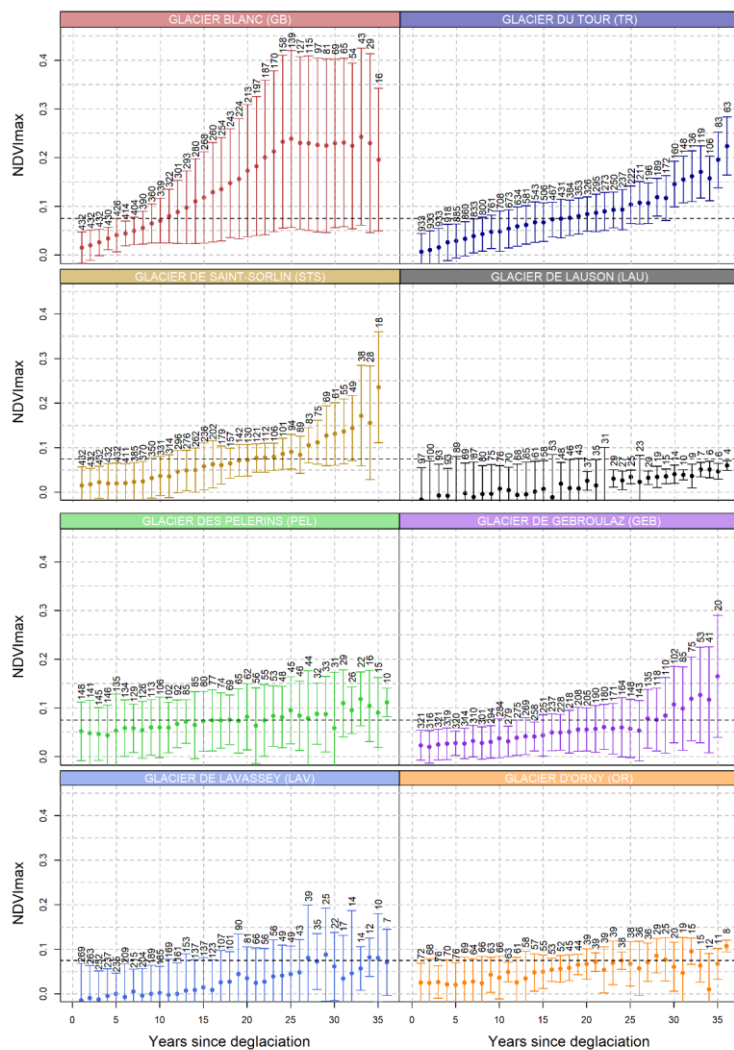
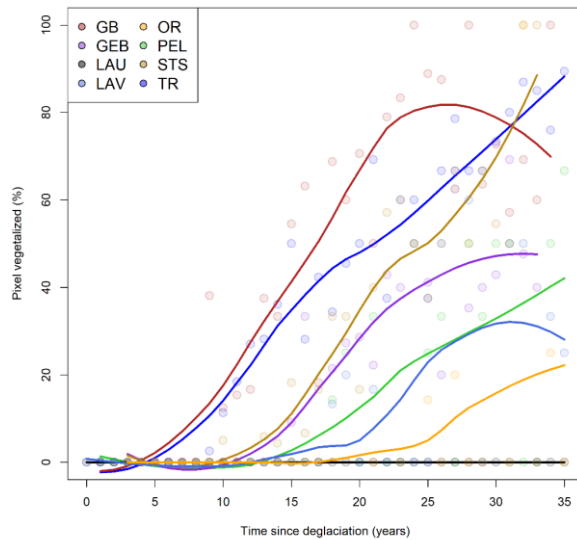


**Figure 3.** (A) Example of indicators derived from the Landsat-based NDVImax time series and deglaciation data for a single pixel located in the Glacier Blanc forefield (latitude: 44.932938 and longitude: 6.409681). (B) Time Lag (TL) and (C) Growth Rate (GR) for an NDVI threshold of 0.75 for the eight margins according to year of deglaciation. Thick black lines represent the median value for each year of deglaciation used to compute anomalies. Green shaded areas represent faster colonization and growth rate than average, while slower than average growth rates are indicated by grey-red shaded areas.





834 **Figure 4.** Distribution of NDVImax values according to the number of years since deglaciation for the [eight](#) glacier [forefieldsmargins](#).  
835 Error bars indicate standard deviation and numbers indicate the numbers of pixels for a given number of years since deglaciation. Horizontal  
836 dashed lines show an NDVI of 0.075. Numbers of pixels for each year since deglaciation are indicated above each error bar.



837  
838 **Figure 5.** Proportion of pixels identified as vegetated according to time since deglaciation for all pixels within the [eight](#) glacier forefields.  
839 [Trend](#)[Thick](#) lines are computed from loess function with span = 0.7.

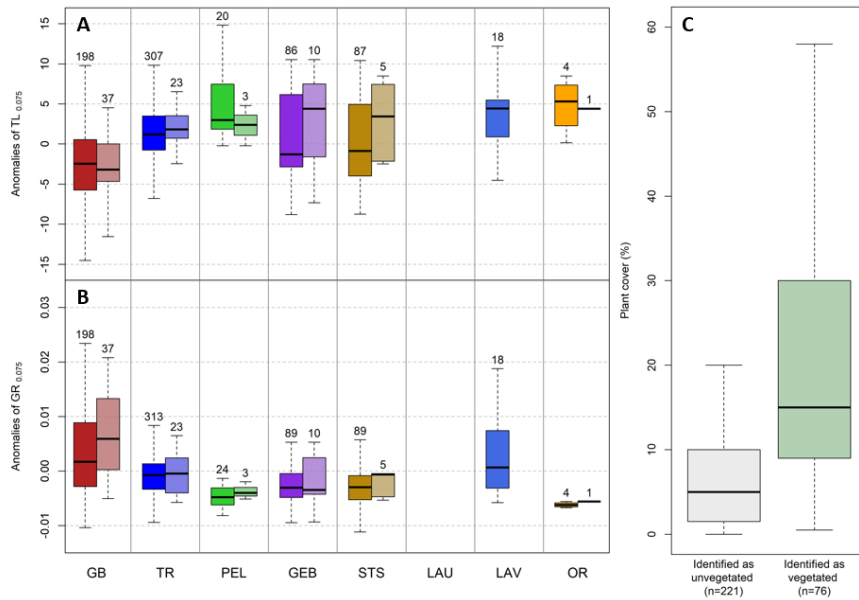


**Figure 6.** Distribution of (A) Time Lag and (B) Growth Rate anomalies for the eight glacier margins for an NDVI threshold of 0.075. For each glacier, the left boxplot with full colours corresponds to all pixels while the right boxplot with shaded colours corresponds only to pixel overlapping floristic plots. (C) Distribution of plant cover (%) for floristic plots that have been identified as vegetated/unvegetated based on the remote sensing approach.

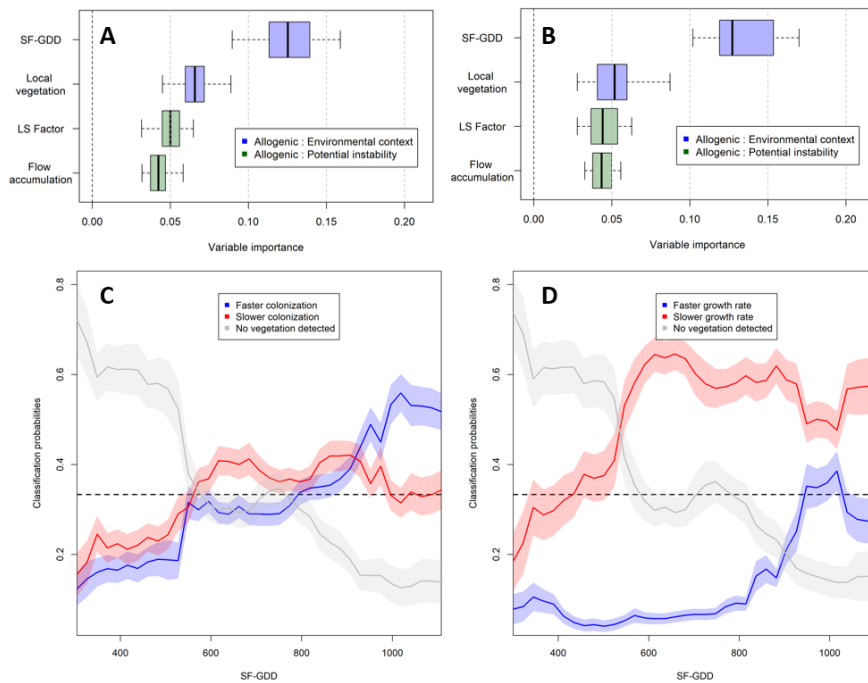


**Figure 7.** Variable importance from the random forest model considering the three classes of (A) TL and (B) GR. Partial dependency plots illustrating how SF-GDD affects class probability for the three classes of (C) TL and (D) GR.

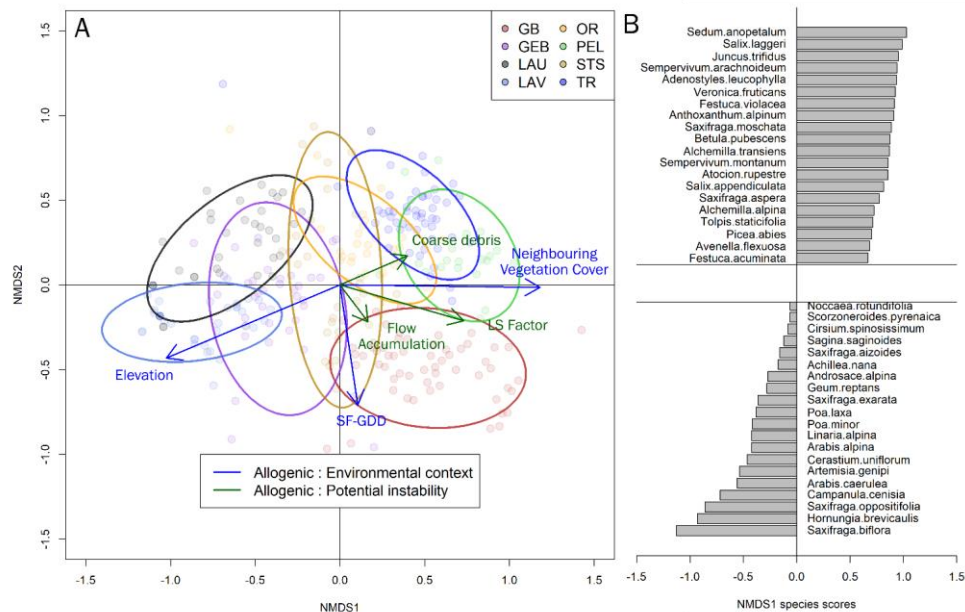


**Figure 8.** (A) Non-metric Multidimensional Scaling (NMDS) of floristic plots by species with vector fitting of explanatory variables implemented using Generalized Least Square (GLS) regression corrected for autocorrelated error structure. Ellipsoids correspond to an interval of 0.8 the standard deviation. The analysis includes 297 plots from the eight glacier forefields. (B) Species distribution along the NMDS axis 1 with the 20 species depicting the highest and lowest scores.

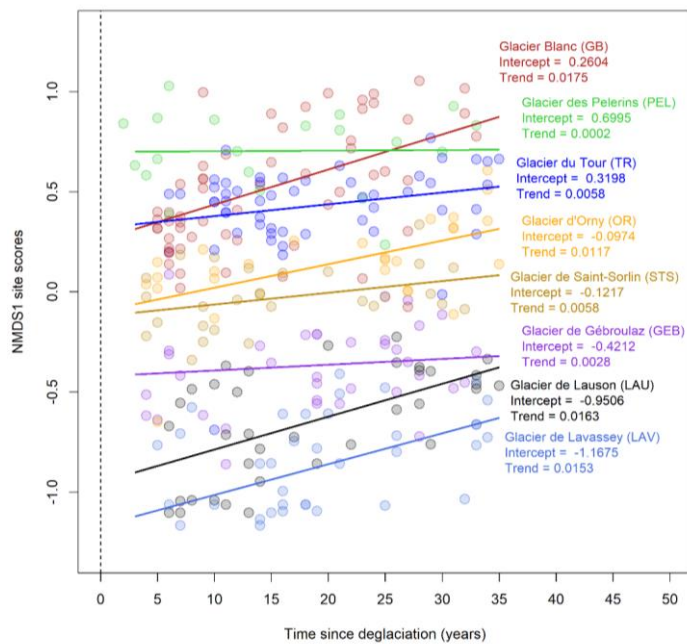


**Figure 9.** First axis scores of the NMDS according to time since deglaciation for the eight glacier forefields. Intercept and slope parameters are shown for each glacier forefield.

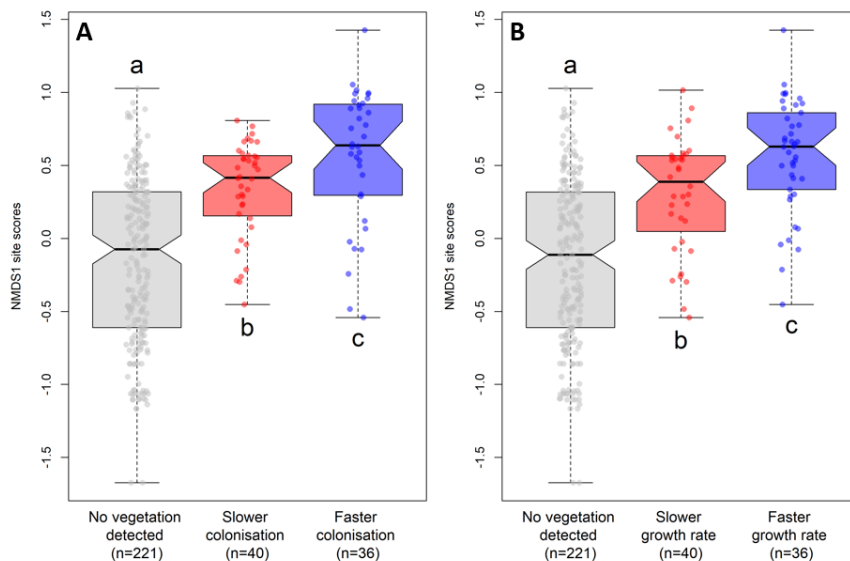


**Figure 10.** First axis scores of the NMDS according to the three classes of anomalies of (A) Time Lag and (B) Growth Rate for an NDVI threshold of 0.075. Letters a, b and c indicate significant differences based on the Wilcoxon test (P-values < 0.05).

<u>Variables set</u>	<u>Variables</u>	<u>With autocorrelated errors structure</u>		<u>Corrected for autocorrelated errors structure</u>	
		<u>AICc</u>	<u>Pseudo-R<sup>2</sup></u>	<u>AICc</u>	<u>Pseudo-R<sup>2</sup></u>
<u>Environmental context</u>	<u>SF-GDD (°C)</u>	<u>464</u>	<u>0.738</u>	<u>58</u>	<u>0.228</u>
	<u>Elevation (m. a.s.l.)</u>	<u>528</u>	<u>0.674</u>	<u>-1074</u>	<u>0.550</u>
	<u>Neighbouring Vegetation cover (NDVI)</u>	<u>567</u>	<u>0.629</u>	<u>138</u>	<u>0.620</u>
<u>Potential instability</u>	<u>LS Factor (°)</u>	<u>771</u>	<u>0.256</u>	<u>775</u>	<u>0.256</u>
	<u>Coarse debris (cm)</u>	<u>830</u>	<u>0.083</u>	<u>834</u>	<u>0.083</u>

Flow accumulation	846	<u>0.040</u>	<u>623</u>	<u>0.033</u>
-------------------	-----	--------------	------------	--------------

**Table 1.** corrected Akaike Information Criterion and Pseudo-R<sup>2</sup> values for two Generalized Least Square (GLS) regression models including or not the autocorrelated error structure.